Aus der Medizinischen Klinik und Poliklinik Ⅱ

der Ludwig-Maximilians-Universität München

Direktorin: Prof. Dr. med. Julia Mayerle

Depletion of α-SMA+ myofibroblasts aggravates pancreatitis in mice

Dissertation

zum Erwerb des Doktorgrades der Naturwissenschaften

an der Medizinischen Fakultät der

Ludwig-Maximilians-Universität München

vorgelegt von

Prince

aus

Rohtak, India

2024

Mit Genehmigung der Medizinischen Fakultät
der Universität München

Betreuer(in):	Prof. Dr. rer. nat. Sibylle Ziegler
Zweitgutachter(in):	PD Dr. rer. nat. Andreas Herbst
Dekan:	Prof. Dr. med. Thomas Gudermann
Tag der mündlichen Prüfung:	09 Dezember 2024

Table of content

Zusammenfassung

Die Pankreatitis ist eine Erkrankung des exokrinen Pankreas, die durch eine sterile Entzündung und eine systemische Entzündungsreaktion gekennzeichnet ist. Die akute Pankreatitis (AP) ist gekennzeichnet durch die abrupte Freisetzung vorzeitig aktivierter Pankreasproteasen, die die Pankreas-Azinuszellen schädigen und dadurch Entzündungsmediatoren freisetzen. Mehrere Episoden einer AP können zu einer chronischen Pankreatitis (CP) führen und die pankreatischen Sternzellen (*pancreatic stellate cells*, PSCs) aktivieren. Unter normalen, gesunden Bedingungen befinden sich die PSCs in einem inaktiven Zustand, doch bei Verletzungen werden sie aktiviert und nehmen myofibroblastenähnliche Eigenschaften an. Aktivierte PSCs (α-SMA+ Myofibroblasten) überexprimieren das zytoskelettale Protein α-smooth muscle-Aktin (α-SMA) und produzieren überschüssige extrazelluläre Matrixproteine, wie z.B. Kollagene, und treiben darüber die Pankreasfibrose. Darüber hinaus spielen α-SMA+ Myofibroblasten während AP und CP eine immunmodulatorische Rolle. Dennoch bleibt unklar, wie α-SMA+ Myofibroblasten den Schweregrad der Pankreatitis beeinflussen (Inflammation, Gewichtsverlauf, Schmerzen, Pankreasfunktion) In meiner Doktorarbeit untersuchten wir die Rolle der α-SMA+ Myofibroblasten bei der Pankreatitis mit Hilfe von transgenen α-SMA-tk-Tieren. Nach der Depletion von α-SMA+ Myofibroblasten beobachteten wir unerwarteterweise einen signifikanten Anstieg des Schweregrades bereits in der Frühphase (12h) der Erkrankung. Die frühe Deletion führte auch zu einer schweren systemischen proinflammatorischen Reaktion mit akutem Lungenschaden, während der Schweregrad in der Bauchspeicheldrüse während der ersten 48 Stunden der Pankreatitis unbeeinflusst blieb. Die systemische Entzündung wird durch die Freisetzung von IL-6 angetrieben, welches vor allem von α-SMA-negativen PSCs Subpopulationen produziert wird, wie ich *in vitro* zeigen konnte. Zur Untersuchung des Einflusses der Depletion von α-SMA+ Myofibroblasten auf den chronischen Verlauf begannen wir mit der Injektion von ganciclovir (GCV) nach der Erholung von AP, was die α-SMA+ Myofibroblasten

in α-SMA-tk-Mäusen reduzierte und folglich die Pankreasfibrose verringerte. Die Reduktion der Pankreasfibrose führte nicht zu einer Verbesserung des Schweregrads der CP. Die subtotale Depletion der α-SMA+ Myofibroblasten wiederum führte zu einem signifikanten Gewichtsverlust ohne jedoch die Pankreasfunktion negativ zu beeinflussen. Die Verringerung der α-SMA+ Myofibroblasten verbesserte die Glukosekontrolle bei α-SMA-tk-Tieren geringfügig, während die exokrine Funktion unbeeinflusst blieb. Jedoch, führte die Verringerung der α-SMA+ Myofibroblasten Population zu einer erhöhten Schmerzempfindlichkeit zwei und vier Wochen nach Beginn der Versuche. Zusammenfassend lässt sich sagen, dass die aktuelle Studie auf eine bedeutende Rolle der α-SMA+ Myofibroblasten während AP und CP hinweist. α-SMA+ Myofibroblasten modulieren die systemische Entzündungsreaktion und induzieren Lungenschäden während AP. Bei CP führt die Abreicherung von α-SMA+ Myofibroblasten zu einer signifikanten Verringerung der Fibrose, erhöht jedoch die Schmerzempfindlichkeit und den Gewichtsverlust.

Abstract

Pancreatitis is an exocrine pancreas disorder characterized by sterile inflammation accompanied by a systemic inflammatory response. Acute pancreatitis (AP) is marked by the abrupt release of prematurely activated pancreatic proteases damaging pancreatic acinar cells, thus releasing inflammatory mediators. Multiple episodes of AP may result in chronic pancreatitis (CP). Activation of pancreatic stellate cells (PSCs) is a hallmark of pancreatic injury. Under normal healthy conditions, PSCs are present in a quiescent state, but upon injury, they become activated and attain myofibroblasts-like characteristics. Activated PSCs (α-SMA+ myofibroblasts) over-express α-smooth muscle actin (α-SMA), producing excess extracellular matrix proteins, eventually resulting in pancreatic fibrosis. Additionally, α-SMA+ myofibroblasts exhibit an immunomodulatory role during AP and CP. Nevertheless, if and how activation of PSCs and pancreatic fibrosis influences the severity of pancreatitis remains unclear. In my doctoral thesis, I investigated the role of α-SMA+ myofibroblasts in pancreatitis using a transgenic animal strain (α-SMA-tk mouse), that allows depletion of activated PSCs. After the depletion of α-SMA+ myofibroblasts in the acute phase, we observed a significant increase in the early humane endpoint. Early depletion also resulted in severe systemic proinflammatory response during the first 48h of pancreatitis while not affecting pancreatic damage itself. Systemic inflammation is driven by IL-6 release, causing lung damage in α-SMA-tk animals. *In vitro*, GCV treatment of isolated α-SMA-tk PSCs resulted in higher IL-6 release than WT PSCs, independent of co-culture with macrophages. In CP, we started injecting GCV after recovery from AP, which reduced pancreatic α-SMA+ myofibroblasts in α-SMA-tk mice and, consequently, reduced pancreatic fibrosis. Reduction of pancreatic fibrosis did not improve the severity of CP. In turn, α-SMA+ myofibroblasts reduction caused significant weight loss, however, exocrine function was not impaired. Of interest, the reduction in the α-SMA+ myofibro-

blasts population led to increased pain sensitivity and nerve density in the pancreas. In conclusion, the current study suggests a significant role of activated PSCs and α-SMA+ myofibroblasts during AP and CP. α-SMA+ myofibroblasts modulate the systemic inflammatory response and induce lung damage during AP. In CP, depletion of α-SMA+ myofibroblasts significantly reduces fibrosis but increases pain sensitivity and weight loss.

List of figures

List of tables

List of abbreviations

°C	Degree Celcius
ALI	Acute lung injury
ANOVA	Analysis of variance
AP	Acute pancreatitis
aPSCs	Activated pancreatic stellate cells
BSA	Bovine salt solution
CAMs	Cell adhesion molecules
CARS	Compensatory anti-inflammatory response
CCK	Cholecystokinin
CFTR	Cystic fibrosis transmembrane receptor
COX-2	Cyclooxygenase 2
CP	Chronic pancreatitis
CRBPs	Cellular retinol-binding protein receptors
CTGF	Connective tissue growth factor
DAB	3,3'-diaminobenzadine
DAMPs	Damage-associated molecular patterns
ECM	Excessive extracellular matrix
EGF	Epidermal growth factor
ELISA	Enzyme-linked immunosorbent assay
EMT	Epithelial-to-mesenchymal transition
GBSS	Gay's balanced salt solution
GCV	Ganciclovir
h	Hour
HSV-tk	Herpes simplex 1 virus thymidine kinase
i.p.	Intraparatoneal
IF	Immunofluorescence
IHC	Immunohistochemistry
IL	Interleukin
LPS	Lipopolysaccharide
MCP-1	Monocyte chemoattractant protein-1
MCSF	Macrophage colony-stimulating factor
MMPs	Matrix metalloproteinases
MODS	Multiple organ dysfunction syndrome
MPO	Myeloperoxidase
NF-κB	Nuclear factor kappa B
nm	Nanometer
PAMPs	Pathogen-associated molecular pattern
PBS	Phosphate buffer saline
PDGF	Platelet-derived growth factor
PFA	Paraformaldehyde
PSCs	Pancreatic stellate cells
PSFG	Picrosirius red fast green

qPSCs	Quiescent pancreatic stellate cells
RCF	Relative centrifugal force
RNA	Ribose nucleic acid
RPM	Revolutions Per Minute
SAPE	Sentinel acute pancreatitis event
SEM	Standard error of mean
SIRS	Systemic inflammatory response syndrome
STE	Sodium chloride-tris-EDTA
TGF-β	Transforming growth factor-beta
TIMPs	Tissue inhibitors of matrix metalloproteinases
TLRs	Toll-like receptors
TNF-α	Tumor necrosis factor
TRAIL	TNF-Related apoptosis-inducing ligand
WT	Wild type
α-SMA	Alpha smooth muscle actin

1. Introduction

1.1 Acute pancreatitis

Acute pancreatitis (AP) is an inflammatory condition of the pancreas and one of the common indications for hospital admission [1]. The disease severity ranges from mild and self-limiting to a rapidly progressive disease leading to multiple organ dysfunction syndrome (MODS) [2]. Recent studies have indicated a worldwide increase in the incidence of AP, 4.9-73.4 per 100,000 cases per year. The average mortality rate in severe AP is rapidly approaching 15-20% [3-5]. In patients with necrotizing pancreatitis, the percentage increases up to 40-50% [6, 7]. Various etiologies have been implicated as a trigger for AP, alcohol and gallstones being the most common etiologies in the Western hemisphere [8, 9]. The precise mechanisms by which these factors trigger AP are still unclear. Several explanations have been proposed, but the most common and widely accepted one suggests that pancreatic acinar cell injury permits the premature activation of zymogens (digestive enzymes in the inactive form) in the pancreas. These enzymes damage the pancreas and subsequently initiate autodigestion and immune activation, which finally results in AP and chronic pancreatitis (CP) based on the different factors as indicated in *figure 1*. [10, 11]. Although the pancreas is the primary organ affected in AP, in some cases, the disease can extend to distant organs as a result of systemic inflammation [12]. Studies have highlighted the significance of maintaining the homeostatic equilibrium of pro- and anti-inflammatory cytokine levels to predict the clinical outcome of AP [13, 14]. To date, there are no approved treatment options available for pancreatitis. Thus, understanding the dynamic interaction among immune cells, inflammatory mediators, and signaling pathways in AP is crucial for identifying effective therapeutic strategies.

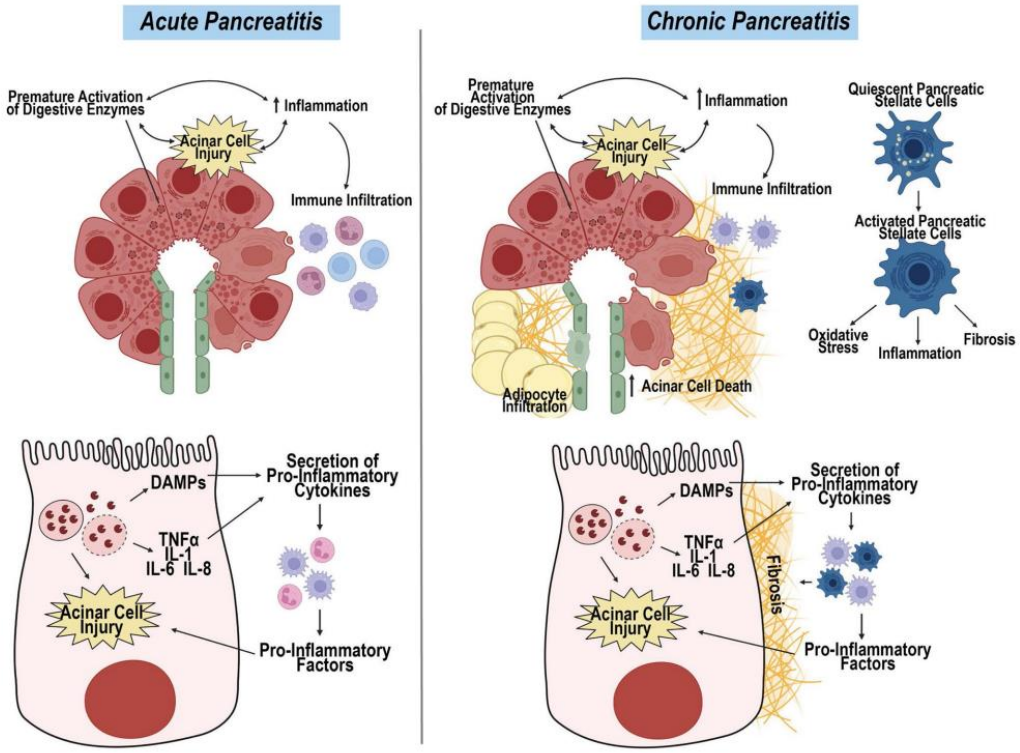

Figure 1: The pathophysiology AP of and CP. *AP arises from acinar injury and pancreatic inflammation, which can be triggered by mechanical obstruction of ducts or systemic factors causing premature activation of digestive enzymes. These stressors induce damage within acinar cells and upregulate the expression of damage-associated molecular patterns (DAMPs), IL-1β, IL-6, IL-8, and TNF-α. Consequently, these molecules are released into the local microenvironment, attracting various immune cells. These immune cells then release additional proinflammatory factors, exacerbating acinar cell injury, which contributes to pancreatic damage progression and systemic injury. CP is a persistent inflammation triggered by various factors, including recurrent AP episodes. Similar to the acute phase, acinar cell injury prompts the expression of proinflammatory cytokines, which stimulate immune infiltration. Besides immunological infiltration, persistent inflammation and cellular stress activate PSCs, leading to increased oxidative stress, inflammation, and fibrosis. This figure is adapted from reference [15] and used under the creative common act.*

1.2 Acute pancreatitis and inflammation

Inflammation is a critical event in the pathogenesis of AP, as the initial release of damage-associated molecular patterns (DAMPs), chemokines, and proinflammatory cytokines by injured acinar elicit an inflammatory response. Accumulating evidence has confirmed that there is a critical role played by inflammatory mediators like interleukin-1 (IL-1), interleukin-6 (IL-

6), tumor necrosis factor-alpha (TNF-α), monocyte chemoattractant protein (MCP-1), and several other cytokines in the induction and severity of AP [16-18]. These responses simultaneously elicit proinflammatory reactions as well as compensatory anti-inflammatory response syndrome (CARS) by release of anti-inflammatory cytokines [19]. This maintains the balance between proinflammatory and anti-inflammatory responses within the body. T-helper-cells appear to be master regulators in the early phase of pancreatitis [13]. Nonetheless, an excessively heightened inflammatory reaction facilitated by the overwhelming release of cytokines and chemokines is coupled with systemic inflammatory response syndrome (SIRS) [20, 21]. Infiltrating neutrophils has been demonstrated to play a crucial role in the early phase of AP and contribute to local and systemic complications [22]. Myeloperoxidase (MPO) is most abundantly expressed in the azurophilic granules of neutrophils and indicates disease severity [23]. The expansion of systemic inflammation during the progression of AP includes diverse pathways and cell signaling systems. Activated macrophages also play a significant role in extending the systemic inflammatory response leading to MODS. Acute lung injury (ALI) is the most common and primary occurring organ dysfunction in AP, and in elderly patients, it accounts for 60% of deaths within the first week after initiation of AP [24, 25].

T lymphocytes, or T cells, are crucial elements of the adaptive immune system that regulate the immune response in pancreatitis. T-helper 1 (Th1) cell population contributes to the inflammatory response by producing cytokines such as interferon-gamma (IFN-γ) and TNF-α, thus exacerbating the severity of AP by promoting inflammatory pathways. In contrast, Th2 cells release cytokines like IL-4 and IL-10, which have anti-inflammatory effects. In AP, the balance between Th1 and Th2 responses is critical. A predominance of Th1 response can lead to excessive inflammation and more severe tissue damage, while a shift toward Th2 responses might help mitigate these effects [13, 26].

As macrophages orchestrate both the initiation and resolution of inflammation, it is clear that the extent of macrophage activation could be one of the critical determinants of the degree of inflammatory response associated with AP [27, 28]. During the transition of AP to CP, there is a dynamic shift in different cell populations, including pancreatic stellate cells (PSCs), as shown in *figure 2*. The role of PSCs in the development of acute pancreatic inflammation remains unknown. However, they have immunomodulatory effects within the pancreas, generating cytokines and chemokines [29, 30]. Thus, they may influence the immunological response by interactions with immune cells like T cells and macrophages [31, 32]. Furthermore, PSCs express MHC class II molecules and may have antigen-presenting capabilities, which aid in developing immune responses specific to particular antigens. It is also known that PSCs have the capacity to control inflammation by secreting pro- and anti-inflammatory mediators. PSCs may help induce immunological tolerance in some cases, but further investigation is needed to thoroughly comprehend how they affect pancreatic diseases, including pancreatitis and pancreatic cancer [33, 34].

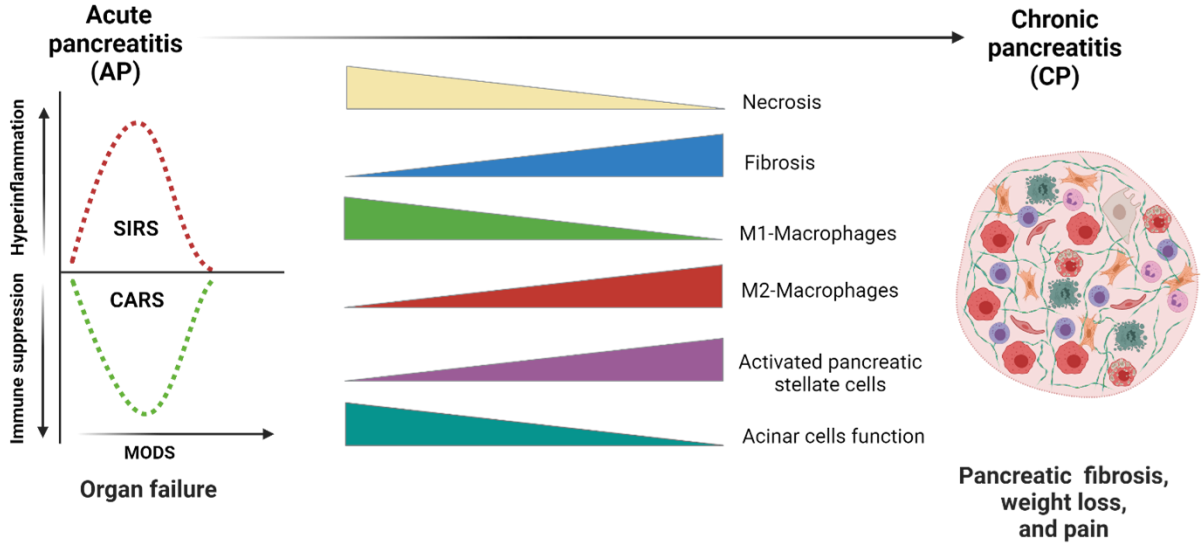

Figure 2: Transition from AP to CP. *AP is characterized by SIRS and CARS, and the disbalance between these two events leads to MODS. Multiple episodes of AP lead to the development of CP, and during this transition, necrosis is replaced by fibrosis. Macrophages play a crucial role in pancreatitis and closely interact with PSCs and other immune cell populations, which*

leads to pancreatic fibrosis that limits the acinar cell function. This diagram is created using BioRender.com

1.3 Acute pancreatitis and multiple organ dysfunction

ALI triggered by pancreatitis can be divided into two stages. Severe alveolar destruction, microvascular injuries, and immune cell infiltration characterize the initial exudative phase. This phase is followed by a fibroproliferative phase. A complex inflammatory cascade recruits more proinflammatory mediators, accelerating the damage. Activated neutrophils, monocytes/macrophages, and mast cells, whether present at the start or recruited later, significantly aggravate the disease. The pathophysiology of lung injury in AP is complex and multifactorial. One mechanism implicated in developing lung complications is the systemic inflammatory response, which can lead to a cascade of events known as a cytokine storm. First-line cytokines, such as IL-1β, IL-6, and TNF-α are released from wounded acinar cells and activate proinflammatory cells. Moreover, macrophages are essential in coordinating the subsequent release of pro- and anti-inflammatory mediators from the liver, peritoneum, and alveolar spaces, and other resident locations. Proinflammatory cytokines, including IL-1β, IL-6, and TNF-α can augment vascular permeability, induce thrombosis, and bleeding, leading to tissue necrosis. Overexpression of adhesion molecules by leukocytes promotes rolling, adhesion, aggregation, and migration toward the injury site [35]. Cytokines further stimulate the upregulation of adhesion molecules, playing a crucial role in pulmonary inflammation and immune response.

1.4 Chronic pancreatitis

CP is a progressive fibroinflammatory syndrome of the pancreas with a complex etiology. It results from repetitive episodes of pancreatitis characterized by inflammation and necrosis resulting in fibrosis. Eventually, it leads to irreversible morphological changes and the permanent loss of endocrine and exocrine functions. Even with the advancement in science, CP is still an

enigmatic disease with undefined pathology, an unpredictable clinical course, and limited therapeutic options. CP is generally linked with clinical complications such as debilitating abdominal pain, endocrine and, exocrine insufficiency accompanied by weight loss, malabsorption, steatorrhea, and brittle diabetes. CP patients are at increased lifetime risk for pancreatic cancer. There are numerous evidence which suggest that there could be more than one etiology present in most of the patients. The TIGAR-O classification system describes the predisposing risk factors, namely toxic-metabolic, idiopathic, genetic, autoimmune, recurrent, and severe AP leading to CP. The TIGAR-O classification system was developed based on an individual risk of having CP is dependent upon more than one risk factor [36]. There are five proposed mechanisms that are responsible for the pathophysiology of CP as described in table 1.

Table 1: Proposed mechanisms for CP pathophysiology.

Mechanism/Factors	Description	References
Necrosis–Fibrosis Sequence Hypothesis	CP develops after repeated episodes of AP, where healing by PSCs and inflammatory cells replace necrotic tissue with fibrotic tissue.	[37]
Sentinel Acute Pancreatitis Event (SAPE) Hypothesis	A single severe AP incident can activate PSCs and cause inflammatory cell infiltration, leading to fibrosis from stress and damage by immune cells.	[38]
Environmental Factors	Toxic metabolites from alcohol, smoking, and tobacco can damage acinar cells.	[15]
Oxidative Stress Mechanism	Free radicals cause oxidative stress in acinar cells, leading to lipid membrane oxidation, cytokine release, and lysosome-zymogen fusion, causing necrosis, inflammation, and fibrosis.	[39]
Ductal Dysfunction	Protein plugs and duct blockages led to reduced bicarbonate secretion from cystic fibrosis transmembrane receptor (CFTR) mutations.	[36, 37]

1.5 Pancreatic stellate cells

In 1982, for the first time, PSCs were discovered, but it took another 15 years until researchers could isolate and culture them. Still, little is known regarding their origin, function, and phenotype in a healthy pancreas [40, 41]. PSCs are resident cells of the exocrine pancreas that account for about 5-7% of the total parenchyma. PSCs and hepatic stellate cells may show functional discrepancies, but they both share 99.9% similarity at the mRNA level, suggesting they might have a common origin [42]. PSCs display a star-shaped cell morphology. These cells are vital for the physiological wound healing response and also serve as storage for vitamin A. Quiescent PSCs (qPSCs) are characterized by an angular shape and abundant cytoplasmic lipid droplets rich in vitamin A. It can be visualized using its auto-fluorescence property if exposed to UV light at 328 nm. Notably, research indicates that vitamin A can impede the activation of epithelial PSCs into mesenchymal myofibroblasts. This potentially inhibits the epithelial-to-mesenchymal transition (EMT) [43].

When exposed to various stimuli such as oxidative stress, inflammatory cytokines, fibrotic growth factors, and toxins, e.g., ethanol or nicotine, PSCs undergo a phenotypic shift from a quiescent stage to an activated myofibroblast-like stage called activated PSCs, the hallmark for which is α-SMA expression. The cytokines and growth factors released by acinar cells, ductal cells, inflammatory cells, or PSCs themselves aid in activating PSCs via autocrine and paracrine stimulation [44]. These activated myofibroblasts are highly mobile and secrete excessive extracellular matrix (ECM). Numerous reports emphasize the significant role of α-SMA+ myofibroblasts in developing pancreatic fibrosis. An imbalance between matrix synthesis and degradation leads to the accumulation of fibrous proteins like type-I collagen and fibronectin, ultimately forming scar [45]. It is unclear whether all α-SMA+ myofibroblasts originate from PSCs or if they are recruited from other mesenchymal tissues to the injury site. There are a

number of different cells that are suspected to be transformed into myofibroblasts, as shown in *figure 3*, and may be involved in fibrogenesis.

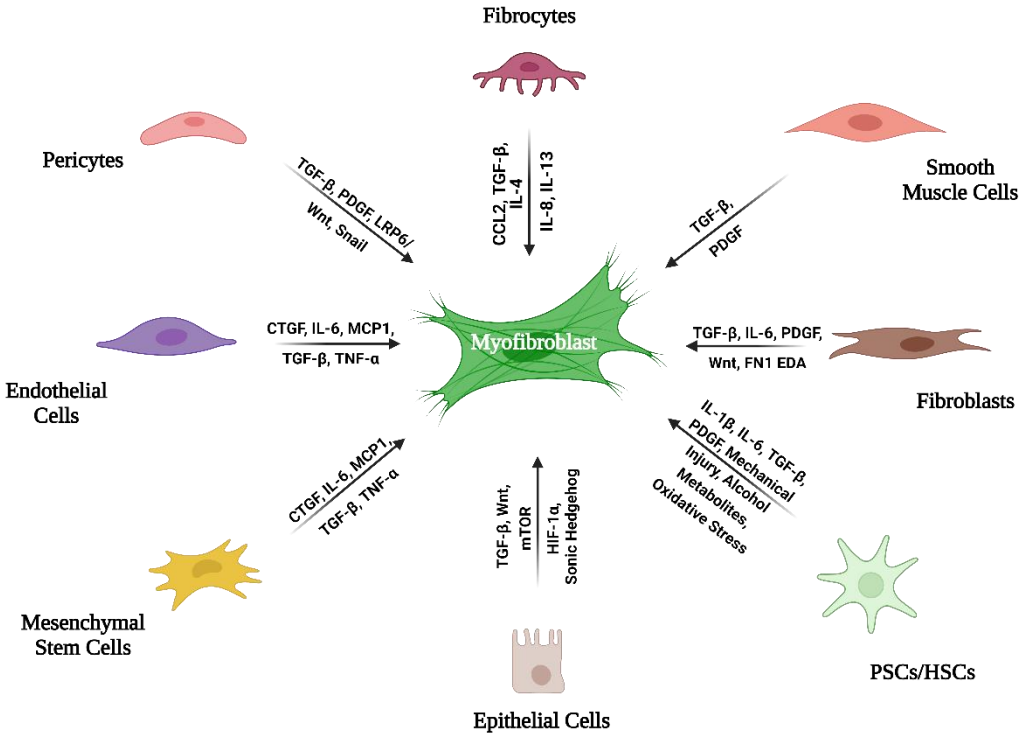

Figure 3: Different cells as a possible source for myofibroblasts transition. *A multitude of cell types residing within the body possess the capability to transform into myofibroblast-like cells under particular pathological conditions, prompted by an array of mediators. These mediators may include growth factors, cytokines, and signaling molecules. This transition to myofibroblast-like cells is often associated with tissue remodeling and repair processes in response to injury or chronic inflammation. This phenomenon is observed across various organ systems, highlighting the versatile nature of these cells and their pivotal role in tissue homeostasis and pathological conditions. This diagram is created using BioRender.com.*

There are numerous lines of evidence linking α-SMA+ myofibroblasts to the development of pancreatic fibrosis through different signaling pathways. It has been demonstrated that platelet-derived growth factor (PDGF) plays an important role in stimulating the proliferation and migration of PSCs. TGF-1, on the other hand, stimulates them to express ECM protein and α-SMA, which acts as a marker for the active and profibrogenic phenotype of PSCs [46, 47]. Apart from producing ECM components, PSCs perform several cellular functions. They also

give rise to matrix metalloproteinases (MMPs) such as MMP-2, MMP-9, and MMP-13, and their inhibitors, tissue inhibitors of metalloproteinases (TIMPs), namely TIMP-1 and TIMP-2. In this way, PSCs synthesize and also degrade ECM proteins, thus, contributing in maintaining the architecture of tissue by balancing matrix [48, 49]. Moreover, PSCs have the ability to perform phagocytosis as well as endocytosis of foreign bodies, old polymorphonuclear cells, and necrotic remnants, suggesting their contribution to the local immune functioning of the pancreas [50].

1.6 Activation of pancreatic stellate cells

Over the decades, it has been studied and focused that qPSCs transformed into activated phenotype (α-SMA+ myofibroblasts). PSCs can be activated directly from the quiescent state or undergo a proliferation state first in response to certain injuries, thus attaining the activated state, as depicted in *figure 4*. The activation of PSCs has been assessed by several features, such as contractility by expression of α-SMA, loss of vitamin A, proliferation, migration, expression and deposition of ECM proteins, and synthesis of MMPs [47, 51, 52]. Activation of PSCs leads to the production of excess ECM, which forms the fibrotic tissue in response to any injury. However, apart from this transformation, other factors are also upregulated during inflammation or injury in the pancreas which are responsible for the activation of PSCs [53]. These include (i) various growth factors, cytokines, chemokines, and proinflammatory mediators, namely IL-6, PDGF, TNF-α, TGF-β, CXCR12, and connective tissue growth factor (CTGF). (ii) Alcoholism and other toxic metabolites such as fatty acid ethyl esters [54]. (iii) Endotoxins such as lipopolysaccharide (LPS), as there is a direct association between circulating LPS and pancreatitis [55]. (iv) Hyperglycemia, as diabetes is associated with the severity of CP [56]. (v) Angiotensin, the renin-angiotensin level is upregulated in pancreatitis [57].

Moreover, there are also other minor components aiding the activation of PSCs such as endothelin 1, cyclooxygenase 2 (COX-2), galectin 1, hypoxia, pigment epithelium-derived factor, fibrinogen, and proteases that get activated during pancreatitis [58-60].

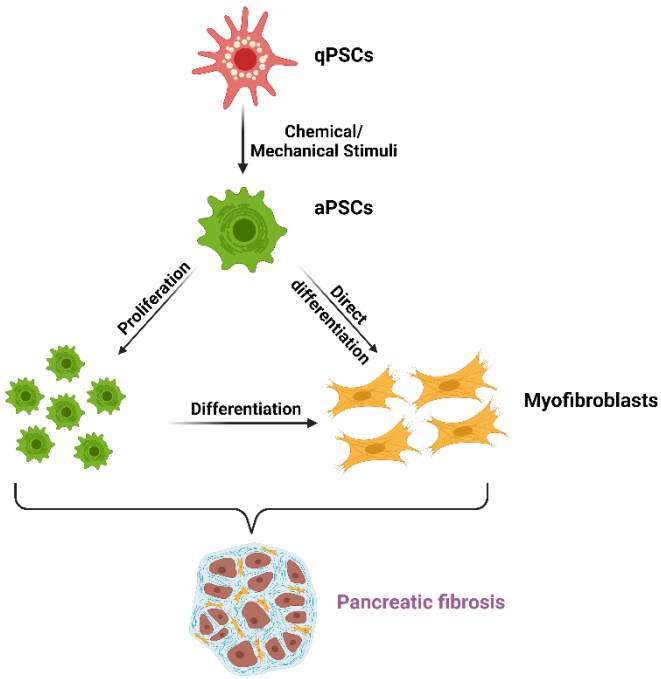

Figure 4: Activation of PSCs. *In response to different stimuli, PSCs become activated, changing from a quiescent state (qPSCs) to an activated state (aPSCs). Once activated, aPSCs are essential for the development of pancreatic fibrosis, which is a defining feature of pancreatic disorders and CP. There are two main ways in which aPSCs can become myofibroblast-like cells: either through a direct process in which aPSCs differentiate into myofibroblast-like cells directly or through an indirect process in which differentiation occurs after proliferation. In pancreatic disorders, both mechanisms exacerbate fibrosis and tissue remodeling by promoting the transformation to myofibroblasts in the pancreas. This diagram is created using BioRender.com.*

1.7 Pancreatic stellate cells and inflammation

Activation of PSCs takes place when exposed to proinflammatory cytokines such as IL-1, IL-6, TNF-α, and the anti-inflammatory cytokine IL-10. All of these mentioned cytokines enhance the expression of α-SMA in PSCs, but their effect on cell proliferation and ECM synthesis varies [61]. During pancreatic injury, IL-6 plays an important role as a regulating factor for activating PSCs [62, 63]. IL-1 enhanced the expression of α-SMA in PSCs *in vitro* did not

affect collagen synthesis and cell proliferation. Recent studies also depicted that during pancreatic injury, TNF-α alone or in association with other factors, such as PDGF, promotes cell proliferation [64]. It has been reported that it may have a role in activating stellate cells and be involved in pathogenesis during pancreatic injury and upregulating cell proliferation and collagen synthesis [65, 66]. Though, it is mainly an anti-inflammatory cytokine whose concentration is known to increase during AP. IL-10 does not affect cell proliferation but upregulates the collagen synthesis by PSCs [67]. It prevents the expression of proinflammatory cytokines, namely IL-8, IL-1, IL-6, and TNF-α, from macrophages. IL-10 is known to possess a protective role during AP. It has been reported that pancreatitis is more severe in IL-10 knockout animals. Upon exogenous administration of IL-10, the severity of pancreatitis was decreased in AP models [68]. The production of proinflammatory cytokines takes place during the initial phase of AP and is present in an increased concentration in blood and in pancreatic tissue. Interestingly, there is an association between the severity of pancreatitis and cytokines concentration, such as the serum level of IL-6, which is considered as a promising clinical biomarker for analyzing the severity in AP [69, 70].

Recently, Aoki *et al.*, observed, an autocrine link among cytokines in PSCs, by demonstrating that the secretion of both IL-1 and IL-6 by PSCs can activate the autocrine secretion of TGF-β, and *vice versa* [71]. Additionally, IL-1, IL-6, IL-13, TNF-α along with MCP-1, stimulate the synthesis of collagen and the expression of α-SMA by α-SMA+ myofibroblasts [47, 72]. Moreover, α-SMA+ myofibroblasts react to paracrine stimulation by external cytokines, and then the cells themselves produce their own cytokines, such as TGF-β, CTGF, MCP-1, IL-1, IL-8, IL-15, and RANTES [73, 74]. All these discussed proinflammatory cytokines may possess antagonistic, synergistic, or complementary effects on PSCs. Alone, TNF-α or IL-1 shows a

mitogenic effect, while the association of both possesses an anti-proliferative effect on fibroblasts [75]. Therefore, the final response of PSCs can be altered due to a combination of these cytokines during pancreatic necro-inflammation.

1.8 Aim of the study

In pancreatitis, PSCs are activated and acquire myofibroblasts-like features that overexpress α-SMA, followed by excess synthesis of ECM proteins such as collagen, leading to pancreatic fibrosis. Activated PSCs (α-SMA+ myofibroblasts) exhibit immunomodulatory role in AP and CP. This thesis investigates the role of α-SMA+ cells in pancreatitis, focusing on their impact on inflammation and fibrosis, and evaluates their potential as therapeutic targets. Using the α-SMA-tk transgenic mice, I investigated the effect of targeted depletion of α-SMA+ myofibroblasts on the severity of pancreatitis as depicted in *figure 5* with following objectives,

Objectives:

A) To investigate whether α-SMA+ cells contribute to acute inflammation by assessing their potential as an independent inflammatory counterpart, and determine their role in exacerbating disease severity. The overall goal is to elucidate whether targeting α-SMA+ cells could represent a viable therapeutic strategy in managing AP.

B) To investigate the role of α-SMA+ cells in promoting pancreatic fibrosis during CP. This part aim to address the unresolved question of whether fibrosis, characterized by inert scarring, contains inflammation and thereby potentially benefits tissue integrity, or if it perpetuates an ongoing inflammatory process that contributes to pancreatic damage. This objective involves depletion of α-SMA+ cells and comprehensively characterizing associated symptoms to elucidate the therapeutic potential of targeting α-SMA+ cells in managing CP.

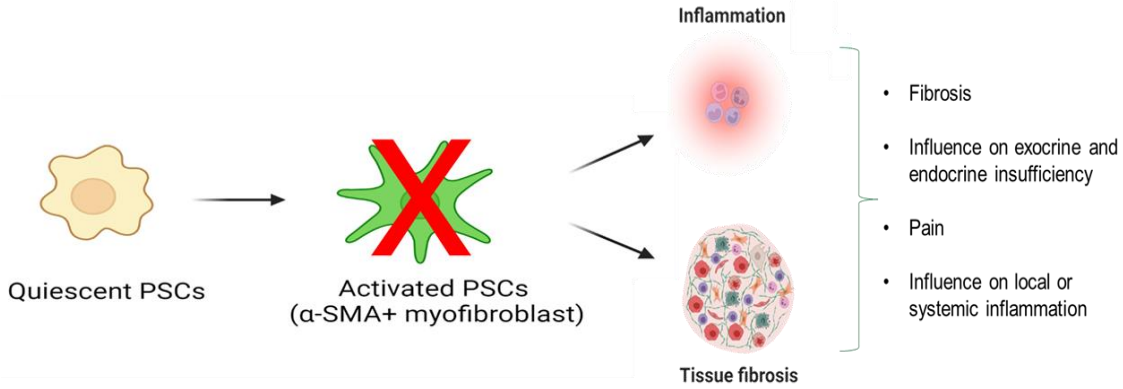

Figure 5: Study hypothesis. *In a healthy pancreas, PSCs typically remain in a quiescent state. However, upon injury, they get activated and attain myofibroblasts-like features, including the overexpression of α-SMA protein. α-SMA+ myofibroblasts interact with other immune cells, exhibit immunomodulatory roles, and synthesize excess ECM proteins, leading to pancreatic fibrosis. Despite their significant impact, the specific role of α-SMA+ myofibroblasts in the context of severity in pancreatitis has never been studied thoroughly. My study aims to address this lacuna by depleting the α-SMA+ myofibroblasts in AP and CP and how the depletion of α-SMA+ myofibroblasts influences the severity of both in AP and CP has been investigated. This diagram is created using BioRender.com.*

2. Material and methods

2.1 Material

2.1.1 Antibodies

Antibodies	Type	Source	Catalog	Manufacturer
Anti-CD3	Primary	Rabbit	ab16669	Abcam, Cambridge, UK
Anti-CD68/F4-80	Primary	Rabbit	MCA49RT	Cell Signaling, USA
Anti-CD45	Primary	Rat	MAB60072	BD Pharmigen
Anti-UCHL1 (PGP9.5)	Primary	Rabbit	13179S	R&D Systems, USA
Anti-CD11b	Primary	Rat	eBio#11-0112-82	Thermo Fisher Scientific, Waltham, USA
Anti-IL6	Primary	Rabbit	ab214429	Abcam, Cambridge, UK
Anti-α-Smooth Muscle Actin	Primary	Rabbit	19245S	Cell Signaling, USA
Anti-Vimentin	Primary	Goat	AF2105	R&D Systems, USA

2.1.2 Enzymes, substrate, and kits

Enzyme or kit	Manufacturer
Cell Counting Kit-8	Abcam, Cambridge, UK Gerbu Biotechnik, Heidelberg, Germany
ELISA MAX™ Standard Set Mouse IL-6	Biolegend, San Diego, CA, USA
LIPC	Roche, Germany
Lipase, *Chromobacterium viscosum*	Merck Chemicals, Darmstadt, Germany
Mouse Cytokine Array C3	Ray Biotech Life, Inc, GA, USA
Pierce BCA Protein Assay Kit	Thermo Fisher Scientific, Waltham, USA
QUIAEX II (Gel Extraction Kit)	Qiagen, Hilden, Germany
Rhodamine 110	Thermo Fisher Scientific, Waltham, USA

2.1.3 Chemicals

Chemical or reagent	Manufacturer
Albumin fraction V, bovine serum albumin (BSA)	Carl Roth GmbH, Karlsruhe
Ammonium acetate	Sigma-Aldrich, St. Louis, USA
Boric acid	Sigma-Aldrich, St. Louis, USA
Bromophenol blue	Sigma-Aldrich, St. Louis, USA
Calcium chloride ($CaCl_2$)	Sigma-Aldrich, St. Louis, USA
Caerulein	Sigma-Aldrich, St. Louis, USA
Crystal violet	Sigma-Aldrich, St. Louis, USA
DAB substrate kit	Vector Laboratories
DAPI (4′,6-Diamidino-2-phenylindole dihydrochloride)	Sigma-Aldrich, St. Louis, USA
Dimethylformamid (DMF)	Carl Roth GmbH, Karlsruhe, Germany
Dimethyl sulfoxide (DMSO)	Sigma-Aldrich, St. Louis, USA
Disodium hydrogen phosphate (Na_2HPO_4)	Carl Roth GmbH, Karlsruhe, Germany
DNA Loading Dye (6X)	Thermo Fisher Scientific, Waltham, USA
Dulbecco's Modified Eagle's Medium (DMEM), high glucose with L glutamine	Sigma-Aldrich, St. Louis, USA
Eosin	Sigma (Taufkirchen, Deutschland)
Ethanol	Merck, Darmstadt, Germany
Fetal Bovine Serum (FBS)	Sigma-Aldrich, St. Louis, USA
GeneRuler Low Range DNA Ladder (10 - 1000 bp)	Thermo Fisher Scientific, Waltham, USA
Glacial acetic acid	Carl Roth GmbH, Karlsruhe, Germany
Glucose	SERVA, Heidelberg, Germany
Glycerol	Carl Roth GmbH, Karlsruhe, Germany
Glycine	Carl Roth GmbH, Karlsruhe, Germany
Hämatoxylin	Sigma (Taufkirchen, Deutschland)

HEPES (4-(2-hydroxyethyl)-1-piperazine-ethanesulfonic acid)	Pan-Biotech, Aidenbach, Germany
Ketamine 10%	WDT, Germany
Magnesium chloride ($MgCl_2$)	Carl Roth GmbH, Karlsruhe, Germany
Methanol	Merck, Darmstadt, Germany
Nuclease free water	Ambion, Naugatuck, USA
Penicillin / Streptomycin (P/S) solution	Sigma-Aldrich, St. Louis, USA
Phosphate-buffered saline (1X) (PBS)	Sigma-Aldrich, St. Louis, USA
Potassium chloride (KCl)	Carl Roth GmbH, Karlsruhe, Germany
Sodium azide (NaN_3)	Carl Roth GmbH, Karlsruhe, Germany
Sodium chloride (NaCl)	Carl Roth GmbH, Karlsruhe, Germany
Sodium dihydrogen phosphate (NaH_2PO_4)	Merck, Darmstadt, Germany
Sodium dodecyl sulfate (SDS) pellets	Carl Roth GmbH, Karlsruhe, Germany
Sodium orthovanadate	Sigma-Aldrich, St. Louis, USA
Sodium periodate ($NaIO_4$)	Honeywell, Charlotte, USA
SYBR™ Safe DNA Gel Stain	Thermo Fisher Scientific, Waltham, USA
SYBR™ Safe Green II RNA Gel stain	Thermo Fisher Scientific, Waltham, USA
Tris base	Carl Roth GmbH, Karlsruhe, Germany
Triton™ X-100	Sigma-Aldrich, St. Louis, USA
Trypsin-EDTA solution (10X)	Sigma-Aldrich, St. Louis, USA
Tween®20	Carl Roth GmbH, Karlsruhe, Germany
Xylazine	WDT, Germany
β-mercaptoethanol	Sigma-Aldrich, St. Louis, USA

2.1.4 Buffers

Name	Composition
Gey's Balanced Salt Solution	
Magnesium chloride ($MgCl_2.6H_2O$)	0.21 g/l

Magnesium sulfate ($MgSO_4$)	0.0342 g/l
Potassium chloride (KCl)	0.37 g/l
Sodium bicarbonate ($NaHCO_3$)	2.27 g/l
Potassium dihydrogen phosphate (KH_2PO_4)	0.03 g/l
Sodium chloride (NaCl)	7 g/l
Sodium hydrogen phosphate (Na_2HPO_4)	0.112 g/l
Calcium chloride ($CaCl_2$)	0.225 g/l
Enzyme solution in GBSS + NaCl	
Collagenase P	1.3 mg/ml
Protease	1 mg/ml
Deoxyribonuclease	0.01 mg/ml
Erythrocyte lysis buffer (10 x)	
H_2O	
Ammonium chloride (NH_4Cl)	1.5 M
Potassium bicarbonate ($KHCO_3$)	0.1M
Ethylenediaminetetracetic acid disodium (EDTA)	10mM
FACS buffer	
PBS	
Sodium azide (NaN_3)	0.02%
Fetal Calf Serum (FCS)	5%
EDTA	2mM
MPO extraction buffer (pH 6.0)	
H_2O	
Potassium dihydrogen phosphate (KH_2PO_4)	50mM
Hexacetyltrimethylammonium bromide	0.5%
MPO-homogenzation buffer (pH 7.4)	
H_2O	
Potassium dihydrogen phosphate (KH_2PO_4)	50mM

STE buffer	
Tris (HCl)	50 mM
NaCl	100 mM
EDTA	1 mM
SDS	1%
TE buffer (pH 7.4)	
Tris (HCl)	10 mM
EDTA	1 mM

2.1.5 Instruments

Equipment	Manufacturer
Branson 450 Digital Sonifier	Marshall Scientific, Hampton, USA
Centrifuge 5417R	Eppendorf, Hamburg, Germany
Centrifuge 5418R	Eppendorf, Hamburg, Germany
Centrifuge 5702R	Eppendorf, Hamburg, Germany
FLUOstar Omega	BMG LABTECH, Ortenberg, Germany
Fusion FX	Vilber Lourmat GmbH, Eberhardzell, Germany
Heracell 240 CO_2 Incubator	Marshall Scientific, Hampton, USA
inoLab pH 720	WTW, Weilheim, Germany
IX50 Phase contrast inverted microscope	Olympus, Shinjuku, Japan
Leica Ctr6000	Leica Microsystems, Wetzlar, Germany
LightCycler® 96	Roche, Basel, Switzerland
Mastercycler® pro vapo.protect	Eppendorf, Hamburg, Germany
Eppendorf Mastercycler® PCR cycle	Eppendorf, Hamburg, Germany
Corning™ Axygen™ Mini Plate Spinner Centrifuge	Corning, New York, USA
Pipetboy acu 2	Integra, Biebertal, Germany

Pipette (10 µL, 100 µL, 200 µL, 1mL)	Eppendorf, Hamburg, Germany
neoLab® Vortex Genie 2, 2700 UpM	NeoLab, Heidelberg, Germany
SpectraMax® Plus 384 Microplate Reader	Molecular Devices, San José, USA
TC20 Automated cell counter	Bio-Rad, Hercules, USA
TS1 ThermoShaker	Biometra GmbH, Göttingen, Germany
IKA magnetic stirrer with heating, RET basic	IKA-Werke, Staufen im Breisgau, Germany
Medingen W22 water bath	Medingen, Preiss-Daimler, Germany
Heraeus HS18/2 Safety extractor hood	Heraeus Instruments, Germany
Digital glucometer	Roche, Basel, Switzerland

2.1.6 Consumables

Material	**Manufacturer**
µ-Slide Chamber Slide (8-well)	Ibidi, Gräfelfing, Germany
Cell culture flasks (25 cm, 75 cm)	Sarstedt, Nürnbrecht, Germany
Cell culture plates (6-well, 24-well)	Greiner Bio-One, Kremsmünster, Austria
Cell culture plates (96-well)	Eppendorf, Berzdorf, Germany
Cell culture plates, TC dish (100 mm)	Sarstedt, Nürnbrecht, Germany
Cryogenic tube (2 ml)	STARLAB, Hamburg, Germany
MultiScreen® IP Filter Plate (96-well)	Merck, Darmstadt, Germany
Ni-NTA HIS sorb plates (96-well)	Qiagen, Hilden, Germany
Nitrocellulose blotting membrane	GE Healthcare, Little Chalfont, UK
PCR reaction tube	Biozym, Oldendorf, Germany
Pipette filter tips (10 µl, 200 µl, 1000 µl)	Sarstedt, Nürnbrecht, Germany
Pipette tips (10 µl, 200 µl, 1000 µl)	Sarstedt, Nürnbrecht, Germany
Reaction tubes (0.5 ml, 1.5 ml, 2 ml)	Eppendorf, Berzdorf, Germany
Reaction tubes (15 ml, 50 ml)	Sarstedt, Nürnbrecht, Germany

Scalpel, Feather disposable scalpel	Feather, Osaka, Japan
Serological pipettes, sterile (5 ml, 10 ml,25 ml)	Sarstedt, Nürnbrecht, Germany
Xtra-Clear Advanced Polyolefin Starseal	STARLAB, Hamburg, Germany
PROLENE® Polypropylene Blue Suture	J& J Medical N.V., Belgium
PERMAHAND® Silk Suture	J& J Medical N.V., Belgium
AutoClip® System	Fine Science Tools Inc. CA USA
Accu-Chek Guide Test Strips	Roche, Basel, Switzerland

2.1.7 Software

Program	**Producer**
Affinity Designer	Serif (Europe) Ltd., Nottingham, UK
EndNote X8	Thomson Reuters, New York City, USA
FCS Express 6 plus Reader	De Novo, Pasadena, USA
FusionCaptAdvance (7.17.02a)	Vilber Lourmat GmbH, Eberhardzell, Germany
GraphPad Prism 10	GraphPad Software, Inc., La Jolla, USA
ImageJ	By Wayne Rasband, NIH, Bethseda, USA
Leica MM AF 1.5	Leica, Wetzlar, Germany
Microsoft Office (Word, Excel, PowerPoint)	Microsoft, Redmond, USA
Omega-Data Analysis	BMG Labtech, Ortenberg, Germany
Softmax Pro 7.0	Molecular Devices, San José, USA

2.2 Methods

2.2.1 Animal experiments

All the animal experimental studies were carried out under the guidelines set forth by FELASA (Federation of European Laboratory Animal Science Associations) after approval from the Regierung von Oberbayern (TVA_ROB_55.2-2532.Vet_02-17-85). The report of all animal experiments conducted was performed according to the ARRIVE (Animal Research: Reporting of *In Vivo* Experiments) guidelines. For the animal experiments, I used transgenic α-SMA-tk animals originally developed by Prof. Raghu Kalluri's group at MD Anderson in the USA [76]. A breeding pair of α-SMA-tk animals was generously provided by Prof. Heikenwälder from DKFZ, Heidelberg. Both male and female α-SMA-tk and wild-type (WT) animals with BALB/c background, aged around 6-8 weeks, were procured from our in-house animal facility. Additional WT controls were purchased from Charles River Inc. All the experiments were carried out at University Hospital, LMU, Großhadern, Munich, Germany.

2.2.2 α-SMA-tk mouse model to deplete α-SMA+ myofibroblasts

Truncated herpes simplex 1 virus thymidine kinase (HSV-tk) is expressed in α-SMA-tk mice, driven by the mouse *α-SMA* gene promoter [77, 78]. When given ganciclovir (GCV), a guanosine analog, this strain of mice permits the ablation of proliferating myofibroblasts that are expressing α-SMA protein. GCV is used as a prodrug in HSV-tk-transfected cells to induce cell death. GCV is phosphorylated by HSV-tk to GCV-monophosphate, which is then transformed by host kinases into GCV-diphosphate and GCV-triphosphate. Only the GCV-triphosphate form leads to apoptotic cell death due to premature DNA chain termination in cells that are expressing α-SMA *(figure 6).* The specificity and efficiency of this mouse model were well characterized in the kidney fibrosis mouse model. Notably, the α-SMA-tk depletion affects the cells showing increased α-SMA-promoter activity and selectively kills these cells.

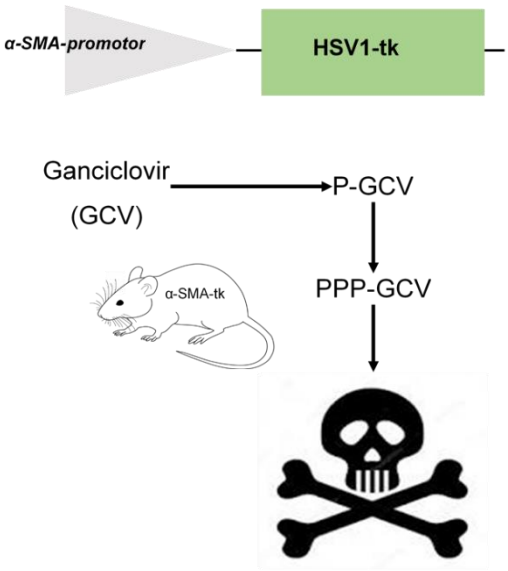

Figure 6: Schematic outlook of α-SMA-tk mouse model.

2.2.3 Genotyping

For genotyping, an ear punch as a biopsy was provided for each animal by the animal breeding facility. DNA extraction from the obtained biopsy was processed using the following protocol. Biopsies were treated with 500 µl of STE-buffer containing proteinase K (20 µg/mL) followed by an overnight incubation at 45°C with a shaking speed of 350 rpm. On the next day, the digested samples were centrifuged at 10,000 rpm for 5 minutes and the resulting supernatant was carefully collected into a new tube. Isopropanol was added to the supernatant and gently rotated for DNA precipitation. The samples were centrifuged for 20 minutes at 4°C with maximum speed to pellet down the DNA. The supernatant was decanted, and a 500 µL volume of 70% ethanol was used to wash the DNA pellet. Following the gentle ethanol aspiration, the DNA pellet from each sample was then dried at room temperature or in a 37°C incubator until complete ethanol evaporation was achieved. Depending on the size of the DNA pellet, it was dissolved in 20–50 µL of ddH_2O. PCR was performed using a validated protocol provided by Jackson Laboratory: denaturing the DNA at 94°C for 4 minutes, followed by a first round of 12 cycles with 94°C for 30 seconds, 64°C for 30 seconds (−0.5°C per cycle), 72°C for 60 seconds and then a second round of 35 cycles at 72°C for 60 seconds and a final extension step

at 72°C for 10 minutes. The WT and α-SMA-tk animals were detected using following primers 5′- TTGAGAACTGTGGAGAGCCTCCAGC-3′ (forward), 5′-GCTGTGATCATGTAATCTTTCTGCC -3′ (reverse), dTK 5′- ATAAGGCATGCCCATT-GTTATCTGG-3′ for PCR *(figure 7)* [78].

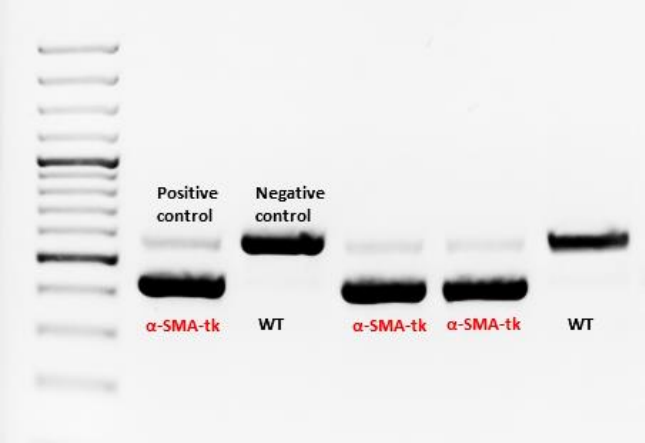

Figure 7: Genotyping of isolated DNA from ear biopsy was performed using PCR. *PCR was performed to determine the presence of the α-SMA-tk gene in newborn mice. Positive and negative controls were used as reference controls.*

2.2.4 Pancreatic duct ligation model for pancreatitis induction

A partial pancreatic duct ligation model was utilized to induce pancreatitis in mice. Animals received atropine as a pre-anesthetic medication 15-20 minutes before the surgical procedure. Anesthesia was induced using a combination of xylazine hydrochloride (2.5-5 mg/kg) and ketamine hydrochloride (100 mg/kg). Under general anesthesia, the animals were positioned on the surgical table in the supine position. The skin was sterilized with 70% alcohol, followed by a clean incision. The head of the pancreas was identified and exposed with a cotton swab. The pancreatic duct was ligated near the head or body part of the pancreas. For the ligation, a surgical thread (4/0 DS19, non-absorbable PVDF thread) was used. The abdominal muscle was then closed with a 7/0 suture (polyester), followed by skin closure using a metal clipper. Animals were exposed to an infrared lamp to maintain their body temperature until the mice woke up. Post-operation pain medication (buprenorphine *i.p.*) was administered, and the animals

were monitored for behavior, posture, movement, and food intake. One to two days after the operation, a single shot of caerulein (50 µg/kg body weight), an analog of cholecystokinin (CCK), was administered, activating protease activity. The animals were housed for different time points based on the experimental setup.

2.2.5 Organ harvest and processing

At the pre-specified time points, the animals were anesthetized using isoflurane. Blood was drawn from each animal and collected in 1.5 mL Eppendorf tubes. The blood tubes were centrifuged, and the obtained sera samples were collected and stored at -80°C for subsequent analyses. Following blood collection, the animals were euthanized via cervical dislocation. Organs, including lungs, liver, pancreas, spleen, and kidneys, were harvested. Small portions of pancreata were preserved in RNAlater solution and stored at -80°C. Rest of pancreata were stored in 4% formaldehyde for histological analysis. One lung lobe was collected from each animal and rapidly frozen for myeloperoxidase (MPO) and cytokine array analysis. Additionally, the spleens were harvested for FACS analyses.

2.2.6 Pancreatic stellate cells isolation

PSCs were isolated from WT and α-SMA-tk animals using the method established by Apte *et al.* [40]. Animals were sacrificed, and the pancreata were harvested quickly and placed in ice-cold saline. Extra fat tissue was removed using a surgical scissor. The pancreata were injected with the enzyme solution containing collagenase P, protease, and DNase. Then, the pancreata were briefly oxygenated and incubated for 4 minutes at 37°C in a shaking water bath with a speed of 160 cycles/minute. After 4 minutes, the shaking speed was reduced to 120 cycles/minute for an additional 3 minutes. Using a surgical scissor, pancreata were finely minced and incubated further for 7 minutes at 37°C with 120 cycles/minutes shaking speed and briefly oxygenated. The cells suspension was filtered through 100 µm nylon mesh. After filtration, the

suspension was centrifuged at 1500 rpm at 4°C for 10 minutes. The supernatant was removed and the cells pellet was resuspended in GBSS + NaCl + 0.3% BSA, followed by centrifugation at 1500 rpm at 4°C for 10 minutes. Following centrifugation, the supernatant was discarded and the pellet was resuspended in 4.5 ml of GBSS + NaCl + 0.3% BSA. To the resuspended pellet, 4 mL of 28.7% nycodenz solution (in GBSS – NaCl) was added. The nycodenz solution was introduced to facilitate cell separation, followed by centrifugation, resulting in a distinctive fuzzy band of stellate cells. These isolated stellate cells were meticulously collected, washed, and cultured in IMDM medium with 10% FBS and 1% Pen-Strep. A healthy pancreas typically yields 5–7% pancreatic stellate cells of total pancreatic cells after isolation.

2.2.7 Macrophage isolation

Macrophage stem cells were isolated from the bone marrow of the femur and tibia of WT and α-SMA-tk animals. For isolation, the bones were dissected and cleaned to remove muscles, tendons, and connective tissue. Then, the joint heads were separated on both sides, and the bone marrow was rinsed in ice-cold PBS. Bone marrow was flushed out into a petri dish using a 23-gauge needle attached to a 10 mL syringe filled with cold PBS. The bone marrow was then pushed through a cell filter (70 µm) to separate the cells. The cell suspension was centrifuged, and the cells were subsequently cultured in RPMI medium containing 10% fetal bovine serum (FBS) and 1% Pen-Strep. After 6h, the medium was aspirated and replaced with fresh medium containing 20 ng/mL macrophage colony-stimulating factor (MCSF). The medium was changed every 2 days. After a week, the cells were confluent and used for further experiments.

2.2.8 Immunofluorescence staining

Cells were fixed with paraformaldehyde for 10 minutes. The fixed samples were washed with PBS. The cells were permeabilized with 0.1% Triton X-100 in PBS for 10 minutes. Subsequently, the samples were incubated in a blocking solution (1% BSA in PBS) for 1h to block nonspecific binding sites. The primary antibody was diluted in the blocking solution and the cells were incubated with the primary antibody overnight at 4°. The next day, the samples were washed thrice with PBS containing 0.05% Tween-20 (PBS-T) for 5 minutes each. The secondary antibody was diluted in a blocking solution, and incubated for 1h at room temperature in the dark. Afterward, the cells were washed thrice with PBS-T for 5 minutes each. The cells were mounted with DAPI-fluorescent mounting medium for 30 minutes. Finally, the slides were allowed to dry, and the cells were visualized using a fluorescence microscope.

2.2.9 Viability assay

Ki8 kit was used to assess the viability of WT and α-SMA-tk cells after GCV treatment. 50,000 cells/well in a 24-well plate and treated with different doses of GCV (0.1, 0.5, 1, 3, and 5 µM) for three days. After three days, 50 µL of Ki8 reagent was added to each well containing 500 µL of media and incubated for 2h at 37°C. After 2h, 100 µL of media was taken from each well, and the absorbance was measured using a spectrophotometer. Percentage cell viability was calculated with respect to untreated control cells and plotted against the different GCV doses. Crystal violet staining was performed to visualize the remaining cells from WT and α-SMA-tk animals after GCV treatment. After three days of GCV treatment, media was discarded, and attached cells were washed with PBS, followed by the fixation with 4% PFA for 15 minutes at room temperature. After 15 minutes, the cells were washed with PBS and incubated with crystal violet dye solution for 20 minutes at room temperature. After 20 minutes, each well was washed gently using tap water until the extra dye was washed off. Then, the plates were dried overnight and scanned with a digital scanner the following day.

2.2.10 FACS

2.2.10.1 Cell isolation from the spleen

First, the entire spleen was placed in 10 mL of PBS. Using a syringe stamp, the spleen was smashed through a 70 µm strainer. The strainer was washed with PBS to ensure all components were collected. The resulting solution was centrifuged at 2800 rcf at 4°C for 5 minutes, and the supernatant was discarded. The pellet was then treated with 5 mL of erythrocyte lysis buffer and incubated for 5 minutes at room temperature. After the incubation, 10 mL of PBS was added, and the solution was centrifuged again at 2800 rcf at 4°C for 5 minutes. The supernatant was discarded, and the pellet was resuspended in 20 mL PBS.

2.2.10.2 Cell staining and flow cytometry

$1x10^6$ cells were stained in a FACS tube for flow cytometric analysis. For this, the cells were first washed and centrifuged at 1200 rpm at 4°C for 6 min in FACS buffer, followed by resuspension and incubation with Fc blocking buffer for 5 min at 4°C. Subsequently, 25 µL of the antibody mixture (in FACS buffer) was added for extracellular staining and incubated for 30 min at 4°C.

After the staining steps, the cells were resuspended in 150 µL FACS buffer, analyzed in a flow cytometer (BD, LSRII), and evaluated with FlowJo. For FACS analyses, the cell suspension was adjusted to $1x10^6$ cells/mL after splenocyte isolation and then passed again through a 70 µm cell sieve.

Table 2: Antibody/dye used for FACS.

Marker	Antibody/dye	Volume of antibody per stain	Catalog number
Live-dead stain	Viability dye	1 µL+332.3 µL in PBS	Thermo L34966
CD45	APC-Cy™7 Rat Anti-Mouse CD45 Clone 30-F11 (RUO)	200 nL/sample	BD 557659 (100mg)
CD3	Brilliant Violet 421™ anti-mouse CD3ε	1000 nL/sample	Biolegend #100336 (500 µL)
CD11b	CD11b Monoclonal Antibody (M1/70), FITC	200 nL/sample	e-bioscience#48-4801
F4/80	F4/80 Monoclonal Antibody (BM8), eFluor™ 450	200 nL/sample	BD 557659 (100mg)

2.2.11 Estimation of serum lipase

Serum lipase activity of acquired animal samples was measured using a LIPC-Cobas kit according to the manufacturer's guidelines. In brief, the serum was diluted in 1:50 dilution in PBS, and subsequently, 10 µL of this dilution was combined with 90 µL of the corresponding substrate. Photometric assessments were carried out in triplicates at 37°C and the kinetics of lipase enzyme activities were analyzed over 30 minutes at a wavelength of 570 nm.

2.2.12 Protein estimation using the Bradford method

The Bradford protein assay was employed for protein quantification. A standard curve was obtained by preparing a set of protein standards with known concentrations. The assay was performed by mixing the protein samples and standards with the Bradford reagent. This was followed by an incubation period of 5-10 minutes at room temperature. Absorbance measurements were then taken at 595 nm using a spectrophotometer [79].

2.2.13 Measurement of MPO activity in lung lysate and serum

To analyze MPO activity, lung samples stored at -80°C were processed for tissue homogenization. This involved mixing the tissue with 500 µL of homogenization buffer and crushing it using a douncer. A 100 µL aliquot of the resulting tissue suspension was extracted for protein determination, subjected to two rounds of sonication for 10 seconds each, and then centrifuged at 10,000 g and 4°C. The remaining 400 µL was centrifuged at 10,000 rcf at 4°C. The supernatant was discarded, and the pellet was treated with 500 µL of extraction buffer. All samples were subjected to four cycles of snap-freezing in liquid nitrogen, followed by thawing at 37°C. After two additional rounds of sonication with 10 seconds each, the samples were centrifuged with 10,000g at 4°C for 10 minutes. The resulting supernatants from each sample were preserved for MPO concentration determination and were stored at -80°C. For MPO determination, 10 µL of the sample was combined with 90 µL of substrate solution (0.167 mg/mL o-dianisidine, 0.21% H_2O_2). Immediate photometric measurement at 460 nm over 10 minutes at 30°C against a standard (purified MPO) was performed for evaluation, focusing on the linear increase in MPO enzyme activity and adjusting it against the respective protein quantity [80].

2.2.14 Cytokine array of lung lysates and serum samples

A cytokines array was performed to quantify the expression of different cytokines in serum and lung lysates. Membranes pre-printed with targeted antibodies were supplied with the kit. 300 µg of protein was used from each sample for incubation with cytokine array membrane. Initially, samples such as serum or tissue lysates were prepared, and their protein concentrations were determined. Subsequently, the array membranes were blocked using a blocking buffer for 30 minutes to prevent unspecific binding. Followed by samples incubation with the membranes overnight. The next day, unbound proteins were removed using wash buffers. The membranes were further incubated overnight with a cocktail of detection antibodies specific to

the target cytokines. The following day, the membranes were washed using wash buffers to eliminate excess antibodies. Chemiluminescent reagents were mixed in equal dilutions to visualize cytokine-antibody complexes and applied over the membranes. The images were captured using the Fusion Vilber imaging system. The expression of different proteins was analyzed using ImageJ Fiji software with a cytokine array plugin. All the raw values were subtracted from the blank sample and finally plotted as a heatmap.

2.2.15 Estimation of fasted blood glucose

Fasted blood glucose was estimated every week using the AccuCheck digital glucometer. All the experimental animals for the chronic phase were fasted for 6h prior to glucose estimation. After 6h of fasting, animals were gently taken out from the cages, followed by tail disinfection. A drop of blood was collected from the tail and directly measured for glucose values.

2.2.16 Estimation of fecal elastase activity

Fecal samples from experimental animals were collected weekly to determine fecal elastase activity by fluorometric enzyme kinetic over an hour at 37°C using Suc-Ala-Ala-Ala-Ala-AMC as a substrate. Stool samples were dried at 37°C and weighed, followed by sonication in fecal sonication buffer containing 500 mmol/L of NaCl, 100 mmol/L of $CaCl_2$, and 0.1% of Triton X-100. After sonication, all the samples were centrifuged at 14000 rpm at 4°C, and stool supernatants were collected in separate tubes. 100 mmol/L Tris, which had $CaCl_2$ concentration of 5 mmol/L with pH adjusted to 8, was used as a substrate buffer. For the final reaction, 10 µL of the sample was combined with 90 µL of substrate solution and enzyme kinetics was determined for an hour at 485/520nm [81]. Blank corrected values were plotted and compared between the two groups.

2.2.17 Pain assessment

2.2.17.1 Open field test

An open field test is commonly utilized as a behavioral test to evaluate general locomotor activity, pain, exploration, and anxiety-like behaviors in rodents [82]. An open field test was performed to assess CP-associated pain in mice in a square box of known dimensions with a digital camera on top of it. The experimental setup was performed in a quiet and well-lit room. Animals were gently placed in the center of the box, and their behavior was recorded using a digital video camera for 5 minutes. The square box floor was wiped with alcohol after each animal, and a black-colored polymer material sheet was used as a contrasting surface. The captured video for each animal was analyzed using ImageJ Fiji software to calculate the total distance traveled in 5 minutes. The final results obtained from different animals were compared based on the groups.

2.2.17.2 Von Frey filament

Hypersensitivity in the abdominal area of the pancreas was assessed in response to Von Frey (vFrey) filaments of different strengths and quantified for nociceptive behaviors. Each vFrey filament exerts a different force against the abdominal wall, as depicted in *table 2.* After an open field test, mice were placed on a wire grid with a mesh opening size of 0.3 mm and covered by a modular animal enclosure box. After an acclimatization time of 5 minutes, filaments of ascending series (from 0.008 to 2 grams) were gently pushed on the abdominal area where the pancreas is located. Each filament was used 10 times within 5–10 seconds, and responses were noted, followed by scorings based on the activity as described in *table 3*. The resulting scores for the 10 stimuli were added and assigned as a total response score [83].

Table 3: Force exerted by different filaments during stimulation to animal.

Target force (grams)	Target force (milliNewtons)	Theoretical pressure (grams/sq. mm)
0.008	0.08	2.53
0.02	0.20	4.39
0.04	0.40	4.93
0.07	0.70	5.53
0.16	1.6	8.77
0.40	3.9	16.1
0.60	5.9	18.4
1.0	9.8	24.4
1.4	13.7	27.9
2.0	19.6	27.4

Table 4: Animals were scored based on their activity during vFrey filament test.

Activity	Response score
No activity	0
Scratching/licking of the stimulated site	1
Jumping or strong reaction	2

2.2.18 Histological evaluation

2.2.18.1 Hematoxylin-eosin staining

For histological evaluation, 2 µm deparaffinized sections were incubated with hematoxylin for 2 minutes, followed by washing under running tap water. The sections were counterstained with eosin for 4 minutes, dehydrated as per standard lab protocol, and fixed in VectaMount

mounting medium. Whole tissue sections were scanned using the Sysmex slide scanner and histological evaluation was performed blindly.

2.2.18.2 Picrosirius red-fast green staining

Picrosirius red-fast green was performed to quantify the fibrosis. Tissue sections of 2 µm thickness were deparaffinized with xylene and in a descending alcohol series. This was followed by incubation at room temperature for an hour with a staining solution of picrosirius red-fast green. It is a mixture of 5 mg direct red 80 dye and 5 mg fast green in 5 mL of picric acid. After incubation, the slides were washed under tap water, followed by dehydration using an ascending series of alcohol gradients. The slide sections were scanned. Collagen-stained fibrosis (red color) and non-collagen-stained healthy (green color) parts were quantified using a pre-trained QuPath model and final values were plotted as a graph.

2.2.18.3 Immunohistochemistry

For immunohistochemistry staining, the 2 µm rehydrated deparaffinized sections were cooked with citrate antigen retrieval buffer for 30 minutes in a pressure cooker. The sections were allowed to cool for 30 minutes at room temperature in the same buffer. The sections were washed with ddH_20 and PBS-T. Afterwards, the slides were treated with 3% H_2O_2 for 20 minutes and then blocked with 1% Aurion BSA for 1h at room temperature. The sections were incubated with respective primary antibodies overnight at 4°C. On the next day, the sections were washed 3 times with PBS-T. Subsequently, HRP-conjugated secondary antibodies were incubated for 1h at room temperature to detect antigen-bound antibodies. Tissue sections were developed using a 3,3'-diaminobenzadine (DAB) Vector peroxidase substrate kit, followed by counterstaining with hematoxylin. The slides were placed under running tap water to wash off

excess hematoxylin. The sections were dehydrated using alcohol gradients and fixed in VectaMount mounting medium. DAB-positive cells were quantified in damaged areas using QuPath software.

2.2.19 Statistical analysis

Data calculations, diagram creation, and statistical analyses were carried out using Microsoft Excel (Microsoft Corporation, Redmond, USA) and GraphPad Prism 10.01 (GraphPad Software, Inc., La Jolla, USA). Flow cytometric analyses were performed with FlowJo V10 (BD Biosciences, Heidelberg, Germany). The evaluation of significant differences was performed using Student's t-test, one-way ANOVA, two-way ANOVA, mixed-effects model, and Bonferroni test with statistical significance set at $p < 0.05$. Results with a p-value below 0.05 were considered statistically significant.

3. Results

3.1 α-SMA+ myofibroblasts are susceptible to GCV treatment *in vitro*

To evaluate the selective cytotoxicity of GCV on α-SMA+ myofibroblasts in α-SMA-tk animals, I isolated PSCs from α-SMA-tk and WT animals. Before conducting the experiments, PSCs were thoroughly characterized. Isolated PSCs displayed prominent lipid droplets, which were clearly visible in both phase-contrast and brightfield images. Immunostaining confirmed that PSCs were positive for desmin and vimentin, markers indicative of quiescent and pan-PSCs, respectively. Upon activation on petri dishes, PSCs predominantly expressed FAP and α-SMA, which are established markers of activated PSCs. Furthermore, activated PSCs began secreting collagen I and III, highlighting their fibrogenic properties. After characterization, cells were cultured on a plastic petri dish, leading to autoactivation and resulting in α-SMA expression. Cells were treated for three days with different concentrations of GCV ranging from 0-5 µM. I observed that the viability of α-SMA+ myofibroblasts isolated from α-SMA-tk animals started reducing from 0.1 µM GCV treatment. WT cells remained viable at 5 µM whereas α-SMA+ myofibroblasts from α-SMA-tk animals reduced by almost 70%. After GCV treatment, cells were stained with crystal violet staining. There was a clear visual difference between WT and α-SMA-tk isolated PSCs in terms of remaining viable cells *(figure 8).*

A)

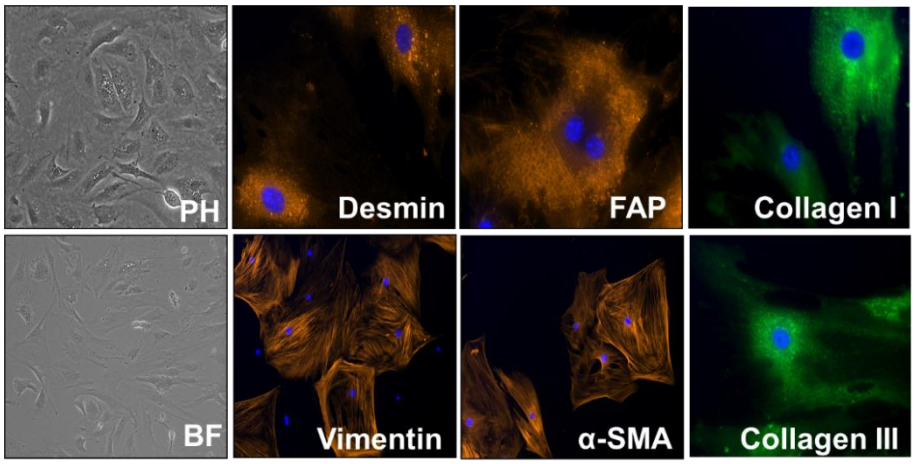

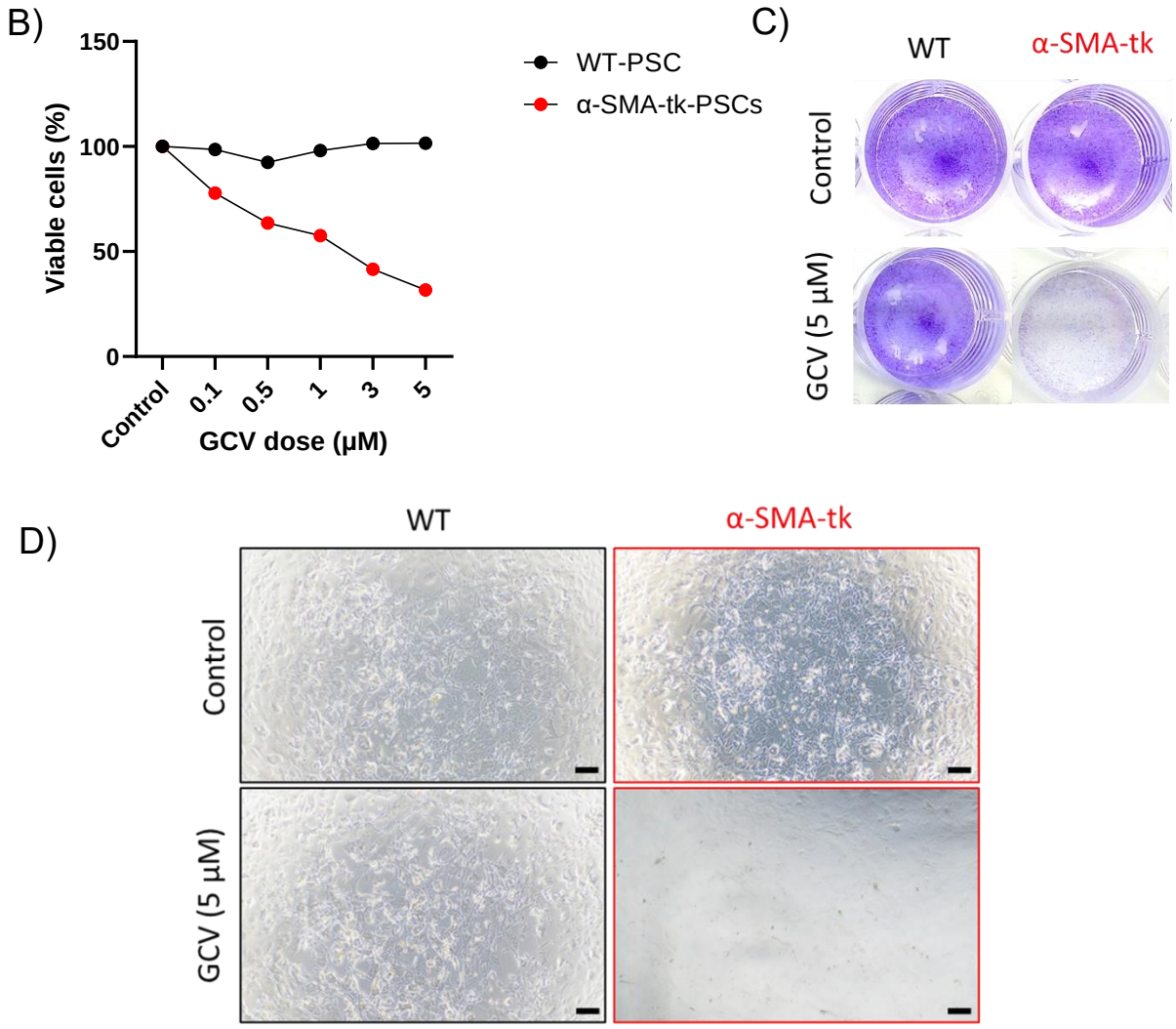

Figure 8: Susceptibility of α-SMA+ myofibroblasts to GCV in vitro. A) Before starting in vitro experiments PSCs were thoroughly characterized by IF staining. B) *α-SMA+ myofibroblasts from α-SMA-tk and WT animals were treated with GCV (0.1, 0.5, 1, 3, and 5* µM*) for 3 days. After 3 days, almost all WT α-SMA+ myofibroblasts remained viable, whereas most of the α-SMA+ myofibroblasts from α-SMA-tk animals did not survive.* ***C)*** *Crystal violet-stained cells after 3 days of GCV treatment (5* µM*).* ***D)*** *Brightfield images of WT and α-SMA-tk PSCs after 3 days of GCV treatment. Values are represented as mean ± SEM.*

3.2 α-SMA+ myofibroblasts ablation causes an early humane endpoint in α-SMA-tk animals

Animals of both groups were treated with GCV (100 mg/kg, *i.p.*) three days before the pancreatic duct ligation, and a single shot of caerulein (50 µg/kg, *i.p.*) was administered one day after surgery. Surprisingly, 90% of the α-SMA-tk group animals reached an early humane endpoint within 24h after caerulein administration, whereas 75% of WT animals survived, as shown in

figure 9. To explore the mechanism behind the excess mortality in α-SMA-tk animals, I slightly modified the animal model for further experiments. In all following experiments, caerulein was injected two days after surgery in order to mitigate disease severity in α-SMA-tk animals. This improved the animal survival, as shown in *figure 9*, and allowed me to study this disease phase in more detail. I observed that delaying the caerulein injection by one day prevented the α-SMA-tk mice from reaching an early humane mortality endpoint, as it allowed for a longer recovery from surgery.

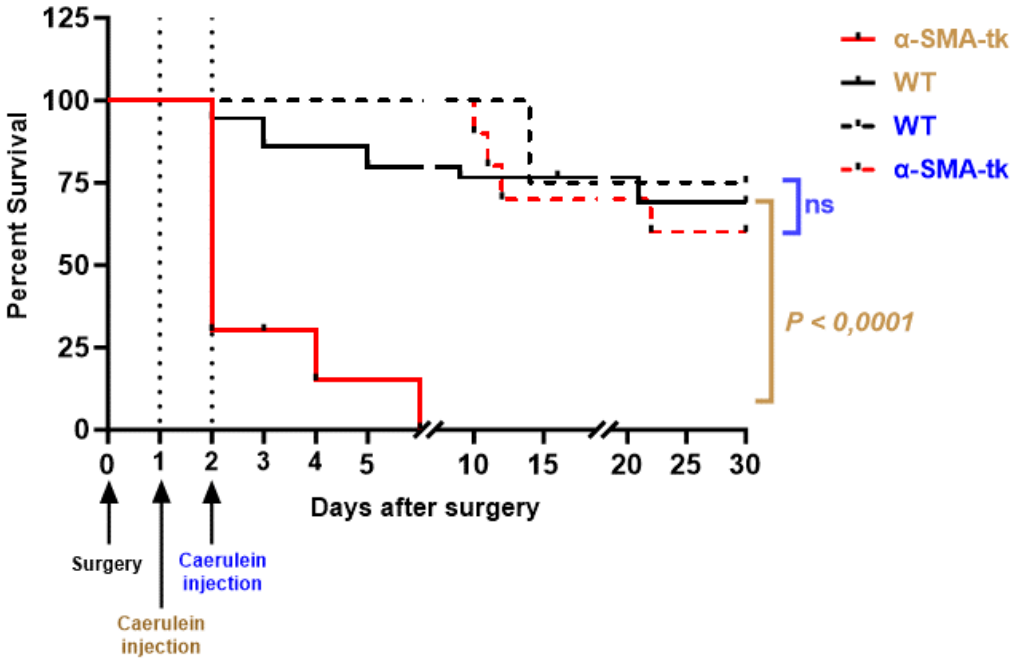

Figure 9: Early depletion of α-SMA+ myofibroblasts in AP causes early humane endpoint. *AP model was developed by performing duct ligation followed by a single injection of caerulein i.p. after 24h from surgery. After pancreatic duct ligation, a significant early humane endpoint was observed in α-SMA-tk animals, but delaying to 48h the caerulein injection prevented the early humane endpoint. Kaplan-Meier test was used for survival analysis (n = 10-48) and p < 0.05 was considered statistically significant.*

3.3 Depletion of α-SMA+ myofibroblasts does not influence local pancreatic damage in AP

To study the consequences of early depletion of α-SMA+ myofibroblasts associated severity in α-SMA-tk mice, I designed early acute phase and late acute phase experiments in which I sacrificed the animals 12h, 24h, and 48h after caerulein injection. It is well-established that the early severity of AP is mediated by a biphasic response. The "first hit" involves the release of premature digestive enzymes, leading to local pancreatic injury. This is followed by the "second hit," characterized by immune cell activation and recruitment, which typically occurs 8–12h after onset. For this reason, animals were sacrificed at the 12h time point to study the early phase. To examine the late acute phase, animals were sacrificed at 24h and 48h. After inducing AP in animals by pancreatic duct ligation, I measured the serum lipase levels to check whether α-SMA+ myofibroblasts have an impact on the severity and pancreatic tissue damage. Surprisingly, I did not find any difference in serum lipase elevation between the two animal groups at different time points of AP *(figure 10).*

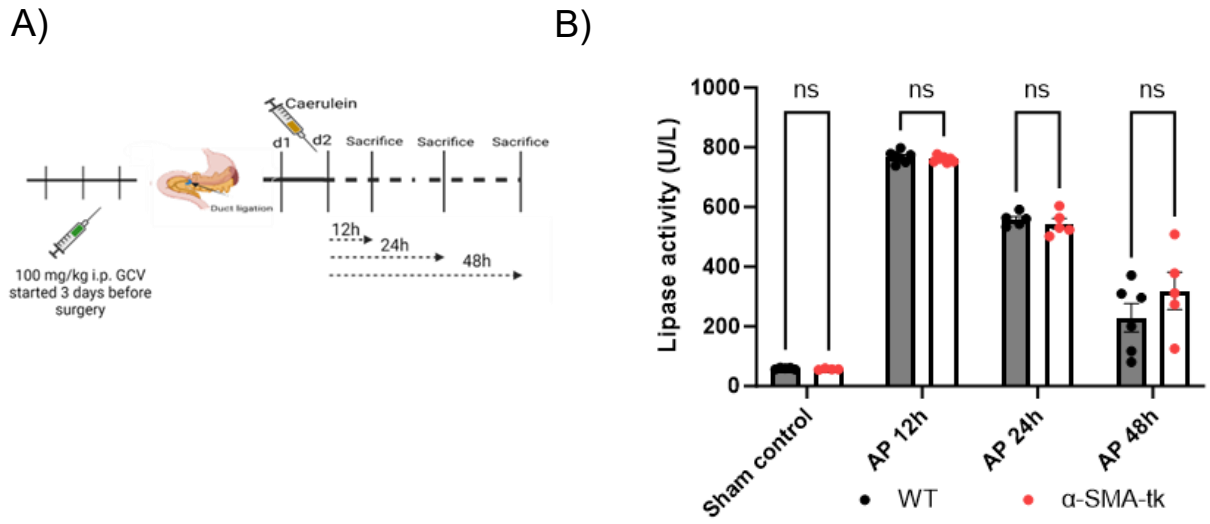

Figure 10: Effect of α-SMA+ myofibroblasts depletion on serum severity marker. A) *Treatment plan for AP**,** the influence of α-SMA+ myofibroblasts on the severity of pancreatitis was analyzed in α-SMA-tk mice by inducing AP using partial duct ligation followed by a single caerulein injection (50 µg/kg) 48h after ligation. Animals of both groups received daily GCV injections (100 mg/kg) started three days before until the end of experiments. Animals were*

sacrificed 12h, 24h, and 48h after the caerulein injection. ***B)*** *Following the duct ligation, there was a sharp increase in serum lipase activity, indicating successful induction of pancreatitis. Depletion of α-SMA+ myofibroblasts did not affect the lipase activity at any time point. 2-way ANOVA followed by Bonferroni multiple comparison test was performed for statistical calculations, and $p < 0.05$ was considered statistically significant. Values are represented as mean ± SEM (n = 3-7).*

Additionally, I evaluated the influence of α-SMA+ myofibroblasts depletion in AP locally in pancreatic tissues in α-SMA-tk animals by using HE, CD45, and F4/80 IHC stainings, as shown in *figure 11*. To my surprise, I did not observe a difference in HE damage scores using the Niederau scoring system [84]. It was conducted by an independent lab member who was blinded to the study groups. Using the QuPath software, I quantified total immune cell populations and found that leukocytes stained with a CD45 antibody remained unaffected between the two groups. Similarly, the F4/80+ macrophages remained unchanged between both groups at different time points of AP (12h, 24h, and 48h). I concluded that depleting α-SMA+ myofibroblasts in the early phase of AP leads to an increase in mortality independent of local pancreatic damage and inflammation.

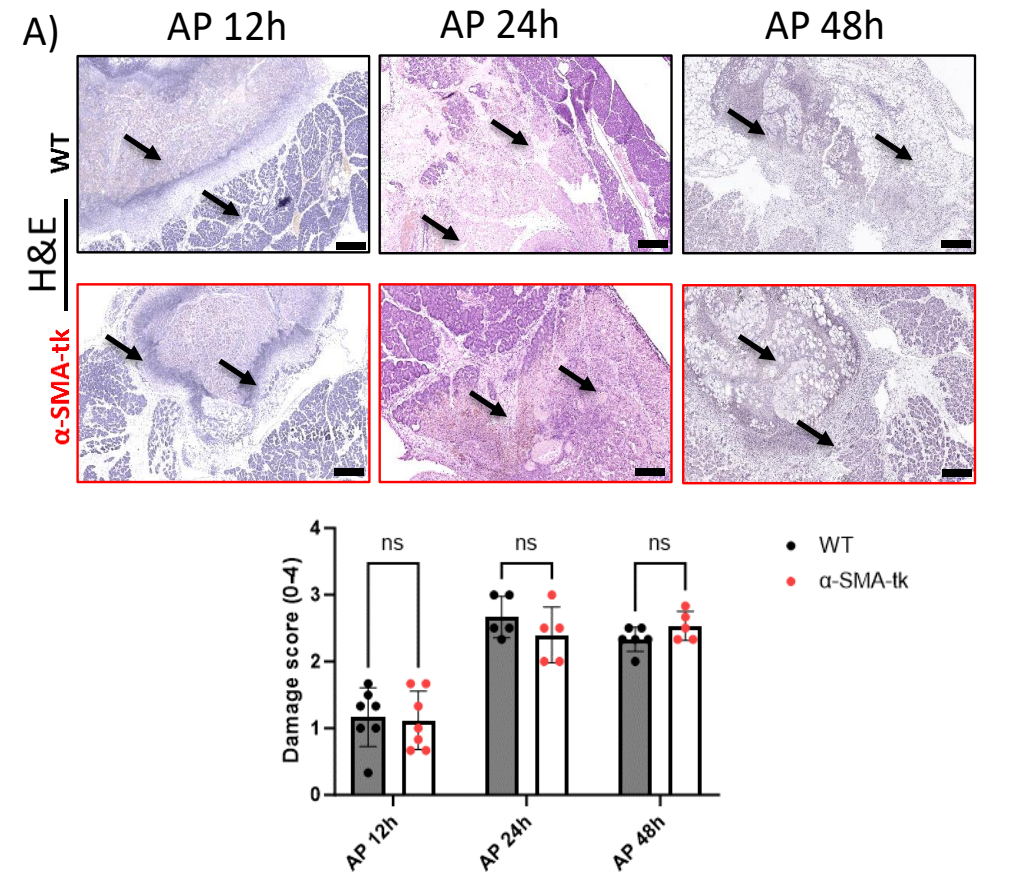
A)
AP 12h
AP 24h
AP 48h
WT
H&E
α-SMA-tk
Damage score (0-4)
ns
ns
ns
WT
α-SMA-tk
AP 12h
AP 24h
AP 48h

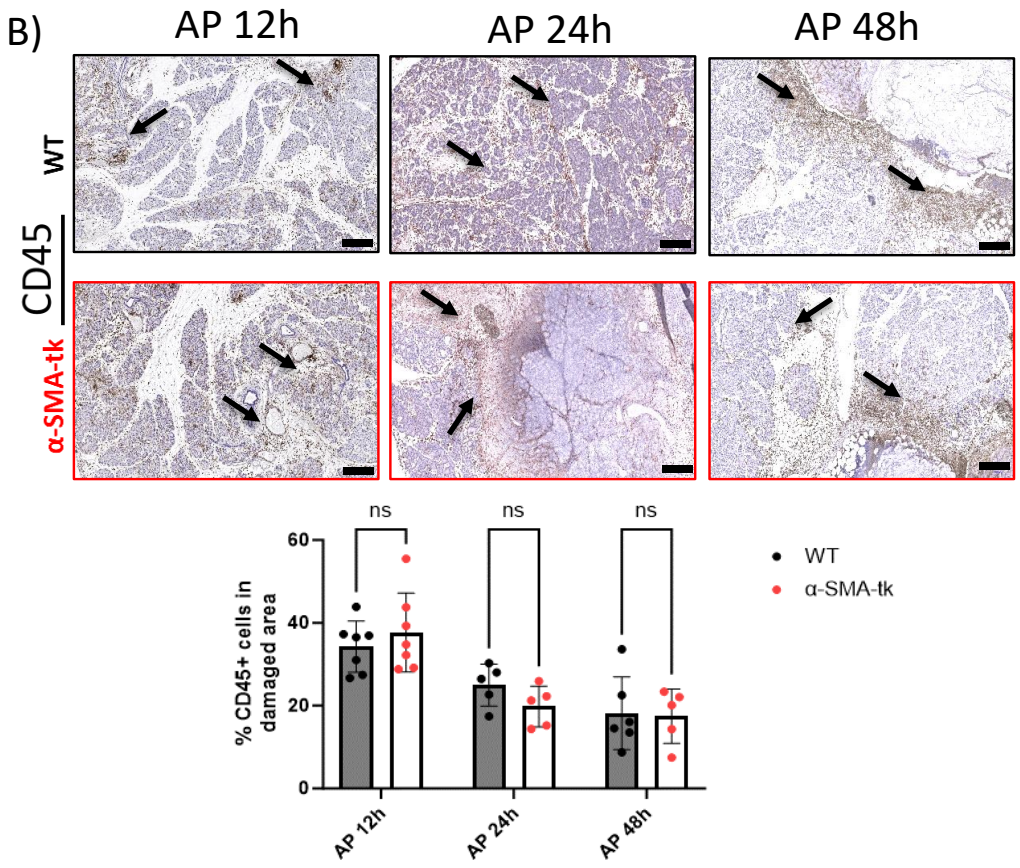
B)
AP 12h
AP 24h
AP 48h
WT
CD45
α-SMA-tk
% CD45+ cells in damaged area
ns
ns
ns
WT
α-SMA-tk
AP 12h
AP 24h
AP 48h

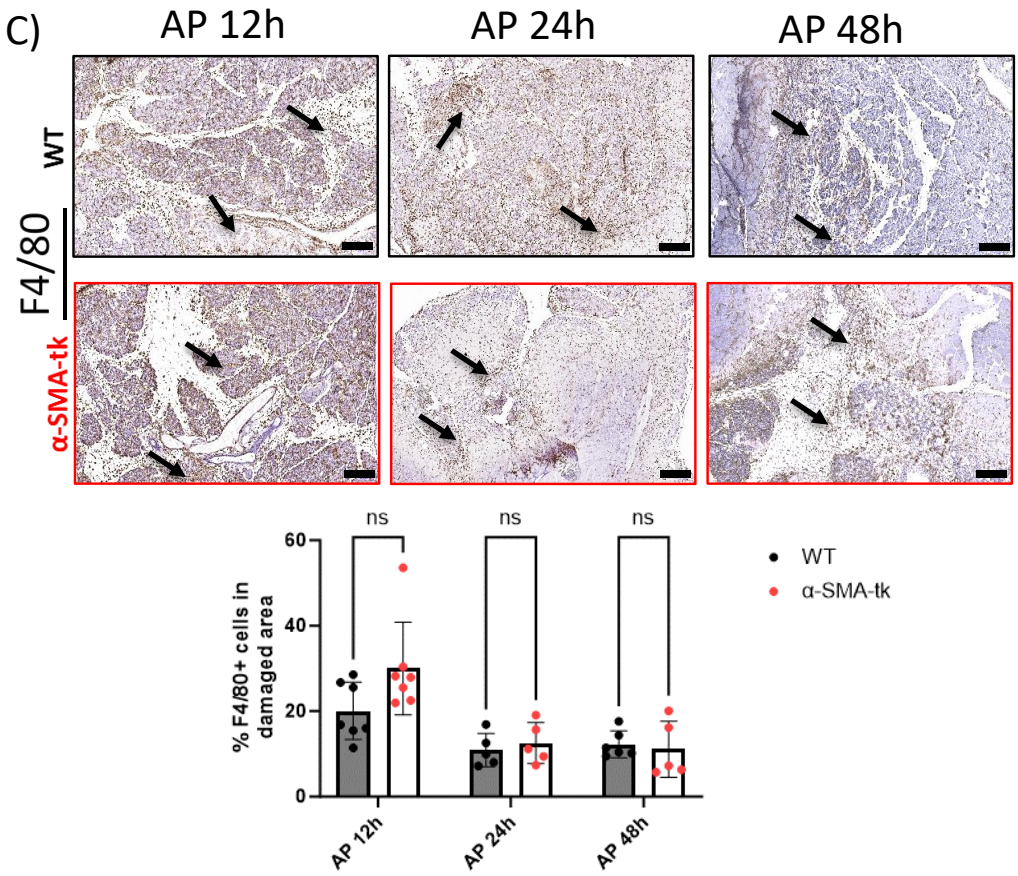

Figure 11: Effect of α-SMA+ myofibroblasts depletion on pancreatic tissue in AP. *AP was induced by partial duct ligation followed by a single shot of caerulein (50 µg/kg) after 2 days. The effect of α-SMA+ myofibroblasts depletion on the severity of pancreatitis in α-SMA-tk animals was assessed. Animals were preloaded with GCV (100 mg/kg, i.p.) 3 days before surgery and continued until the experiments were over. Animals were sacrificed at 12h, 24h, and 48h after caerulein injection. The influence of α-SMA+ myofibroblast depletion on pancreatic damage was assessed by histological stainings.* ***A)*** *H&E staining showed severe necrosis, edema, and inflammation in the pancreas, but there was no difference between the two groups.* ***B)*** *Total immune cells stained with CD45 remained unchanged between both groups.* ***C)*** *Depleting α-SMA+ myofibroblasts did not influence the F4/80+ macrophages. 2-way ANOVA followed by Bonferroni multiple comparison test was performed for statistical calculations, and $p < 0.05$ was considered statistically significant. Values are represented as mean ± SEM (n = 5-7).*

3.4 Depletion of α-SMA+ myofibroblasts provokes a systemic pro-inflammatory response in AP

3.4.1 α-SMA+ myofibroblasts depletion causes severe lung damage in α-SMA-tk animals

Early mortality in the course of severe AP is usually related to MODS. Lungs are the most commonly affected organ in AP and account for significant mortality. I explored the influence of α-SMA+ myofibroblast depletion in AP-associated lung damage in α-SMA-tk animals. I harvested the lungs of AP animals from WT and α-SMA-tk animals and looked for damage in the lungs by assessing histological changes [12]. Interestingly, I found that α-SMA-tk animals had more pronounced damage histologically, as evident by increased alveolar wall thickness and enlarged cell nuclei, as shown in *figure 12*. I further checked the total alveolar space in the whole lung of animals as performed by Glaubitz *et. al.,* using QuPath [14], and found that α-SMA-tk animals at 12h timepoint had significantly reduced alveolar space as compared to WT animals.

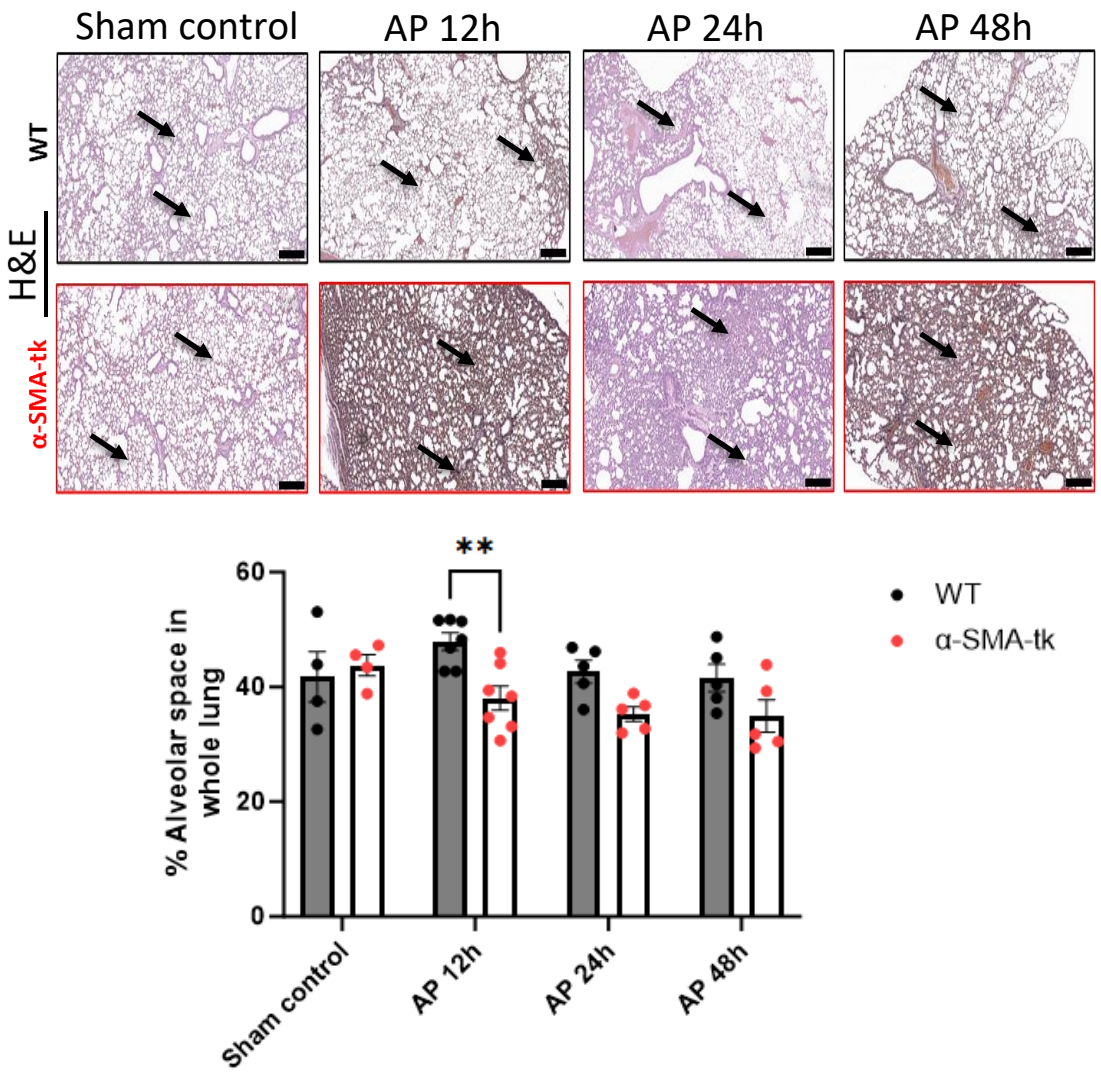

Figure 12: Depletion of α-SMA+ myofibroblasts leads to severe lung damage in AP. *To induce AP, partial pancreatic duct ligation was performed, followed by a single dose of caerulein (50 µg/kg/) after 2 days of duct ligation. Animals were administered GCV (100 mg/kg, i.p.) three days before the surgery and maintained on the GCV throughout the entire experiments. The effect of α-SMA+ myofibroblasts depletion on pancreatitis-associated lung injury was assessed. Animals were sacrificed after 12h, 24h, and 48h of caerulein injection. The depletion of α-SMA+ myofibroblasts resulted in pronounced architectural changes in lungs morphology and a significant reduction ($F = 10.78$, $p < 0.01$) in alveolar space throughout the lungs of α-SMA-tk animals at 12h timepoint. Mixed-effects model followed by Bonferroni multiple comparison test was performed for statistical calculations and $p < 0.05$ was considered statistically significant. Values are represented as mean ± SEM ($n = 4$-7).*

3.4.2 Reduction of α-SMA+ myofibroblasts results in increased MPO level in lungs

I hypothesized that a severe proinflammatory response caused the secondary damage to the lungs by monocytes recruitment, as previously described [80, 85]. The systemic immune response can be determined based on lung MPO activity [14]. I measured the MPO activity in the lung lysates of animals from both groups. I found that α-SMA-tk animals at 12h timepoint had a significantly increased MPO activity in contrast to WT animals, as depicted in *figure 13*. MPO activity peaked at 12h and decreased after in both groups. However, the activity remained higher in the α-SMA-tk animals during 24h and 48h time points. This indicates that monocytes-mediated systemic inflammation was more pronounced in α-SMA+ myofibroblasts depleted animals.

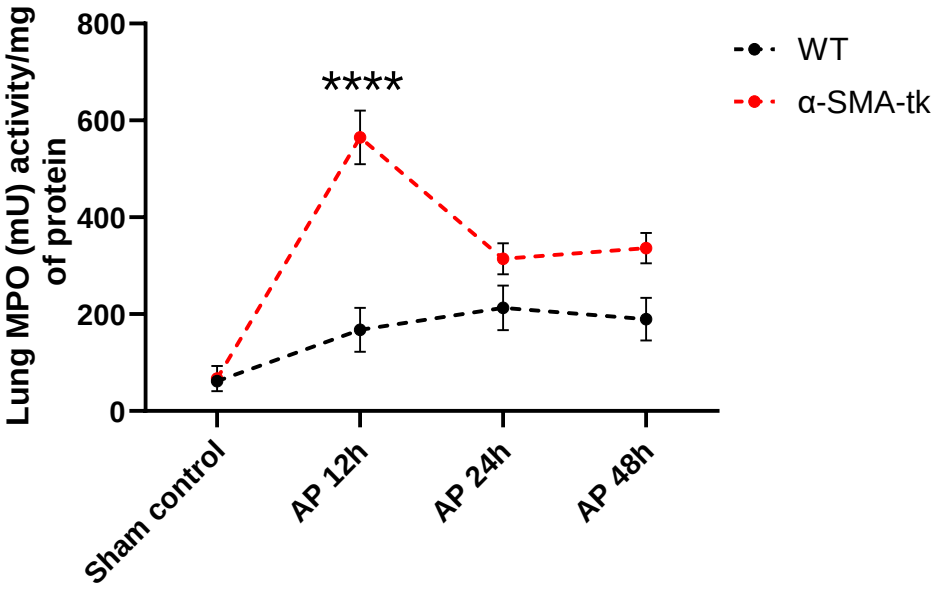

Figure 13: Depletion of α-SMA+ myofibroblasts leads to higher lung MPO activity in AP. *After pancreatitis induction by duct ligation and a single caerulein (50 µg/kg) injection, the animals were sacrificed at 12h, 24h, and 48h time points. The animals were treated with GCV (100 mg/kg, i.p.) three days before duct ligation and until the end of the experiments. The systemic immune response was determined by MPO activity in the lungs. α-SMA+ myofibroblasts depleted animals showed the highest level of lung MPO activity at 12h timepoint ($F = 16.21$, $p < 0.0001$). 2-way ANOVA followed by Bonferroni multiple comparison test was performed*

for statistical calculations, and p < 0.05 was considered statistically significant. Values are represented as mean ± SEM (n = 4-7).

3.4.3 α-SMA+ myofibroblasts depletion leads to an increased macrophage population in splenocytes

Immune cells play an important role in driving the systemic immune response in AP. Using FACS, I explored the dynamics of immune cells in WT and α-SMA-tk animals in an early acute phase time point (12h) from splenocytes, with support from AG Lauber, Department of Radiation Oncology, LMU Munich. I did not find any significant change in the CD45+ total immune cell population in isolated splenocytes of both groups. Furthermore, I observed no difference in the CD3+ T cell population between both groups. Macrophages play a crucial role in SIRS associated with AP. Hence, I quantified the total macrophages population, as shown in *figure 14*. I found that α-SMA-tk animals had a significantly higher population of macrophages in comparison with WT animals.

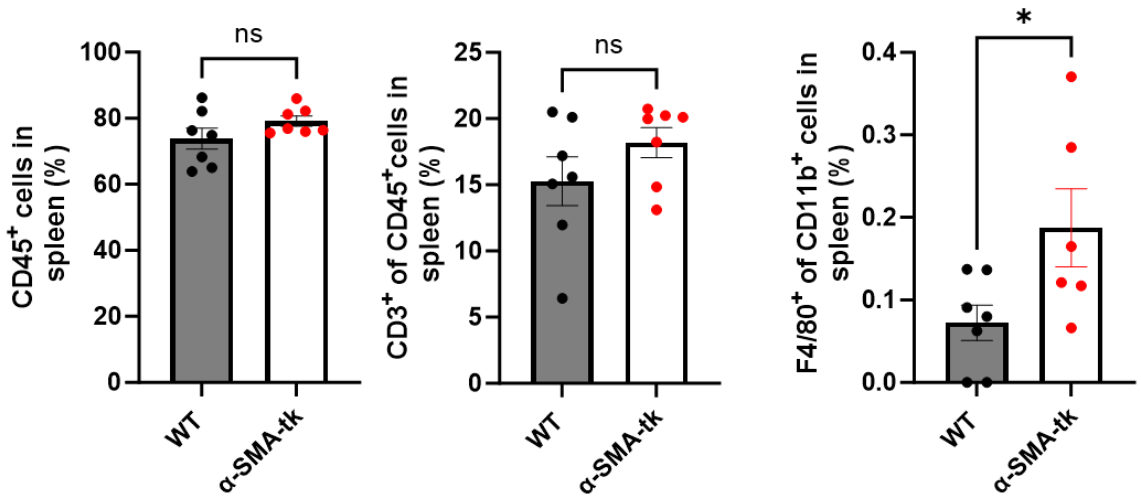

Figure 14: Depletion of α-SMA+ myofibroblasts resulted in a higher macrophage population in AP. *Following the induction of pancreatitis through duct ligation and a single injection of caerulein (50 µg/kg, i.p.), animals were euthanized at 12h time points. Animals were treated with GCV (100 mg/kg, i.p.) three days before surgery and continued until the end of experiments. Flow cytometric staining of isolated splenocytes revealed no changes in the total immune cell population and CD3+ T cells in both groups. However, CD11b+ F4/80+ cells*

showed a significantly higher level in α-SMA+ myofibroblasts depleted animals. Unpaired t-tests were performed for statistical calculations, and p < 0.05 was considered statistically significant. Values are represented as mean ± SEM (n = 6-7).

3.4.4 α-SMA+ myofibroblasts depletion provokes a severe immune response in α-SMA-tk animals

AP leads to pancreatic necrosis, which marks the injury of acinar cells, and damaged acinar cells as well as activated immune cells release cytokines that drive systemic inflammation including pulmonary injury [14]. To investigate different cytokine profiles driving systemic inflammation, I performed a cytokine array for both serum and lung lysate samples of matched animals at a 12h time point. Out of 64 different cytokines, I noticed a significant upregulation of IL-6 cytokine in both serum and lung lysates *(figure 15A).* I also estimated IL-6 level in pancreatic tissue homogenates of the same animals using ELISA. I observed a trend towards higher IL-6 levels in the pancreatic tissues of α-SMA-tk group (*figure 15B).*

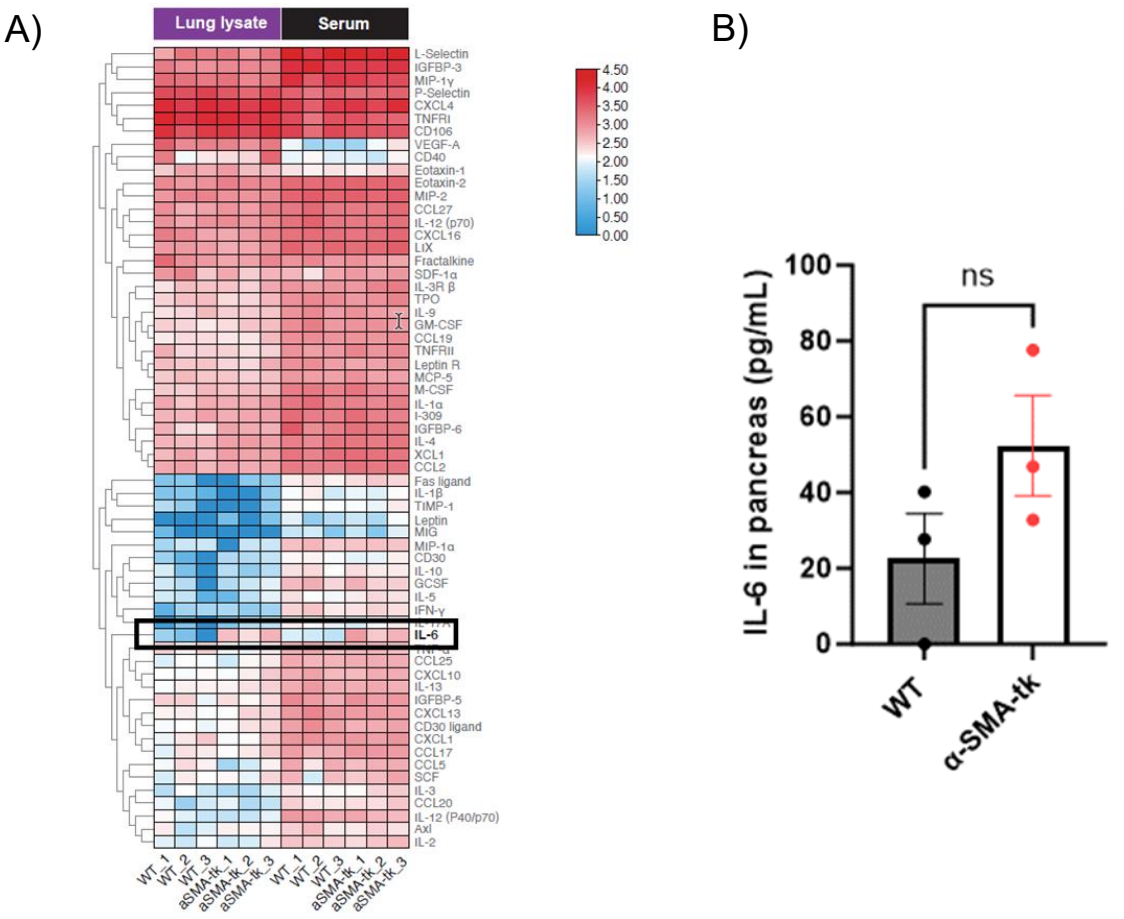

Figure 15: Depletion of α-SMA+ myofibroblasts resulted in higher IL-6 expression in AP. *AP model was developed through duct ligation and the administration of a single caerulein injection (50 µg/kg). GCV (100 mg/kg, i.p.) injection was started 3 days before surgery and continued until the end of the experiment. Animals were euthanized at 12h timepoint after caerulein injection.* ***A)*** *Cytokines array was performed for lung lysate and serum samples of matched animals. Cytokine profiling showed a significantly higher concentration of IL-6 in both lung lysates and serum samples of α-SMA-tk animals.* ***B)*** *Using ELISA, pancreas tissue lysates showed relatively higher expression of IL-6 levels in α-SMA-tk animals. Unpaired t-test was performed for statistical calculations, and $p < 0.05$ was considered statistically significant. Values are represented as mean ± SEM (n = 3).*

3.4.5 α-SMA+ myofibroblasts depletion generates IL-6 *in vitro*

I observed a rise in systemic IL-6 levels *in vivo* without changes in the cellular inflammatory component in the pancreas or systemically. I, therefore, turned to the PSCs themselves, to explore the possible source of IL-6. I performed co-culture experiments with isolated PSCs as well as macrophages from WT and α-SMA-tk animals. Culturing PSCs on plastic plates leads to autoactivation and acquisition of α-SMA+ myofibroblast features. I cultured the macrophages and PSCs from both animal phenotypes separately and also in different co-culture settings with and without GCV. I did not observe a change in IL-6 release comparing WT and α-SMA-tk-PSCs without GCV treatment. I observed a sharp increase in IL-6 release when the α-SMA-tk-PSCs were treated with GCV (5µM) in comparison to WT-PSCs. Similarly, I treated WT- and α-SMA-tk macrophages with and without GCV and did not find any difference between IL-6 release in the supernatant. Additionally, I co-cultured WT-PSCs + WT-macrophages, WT-PSCs + α-SMA-tk-macrophages and vice-versa. I did not find any additional effect in macrophages co-cultured with α-SMA-tk-PSCs on IL-6 release when compared to PSCs alone as shown in *figure 16.* These results suggest that an α-SMA-negative PSCs subtype and not inflammatory cells are responsible for IL-6 release during early AP and that α-SMA+ myofibroblasts are protective during a phase of systemic hyperinflammation in AP. Further characterizing these PSCs subtypes was beyond the scope of my thesis.

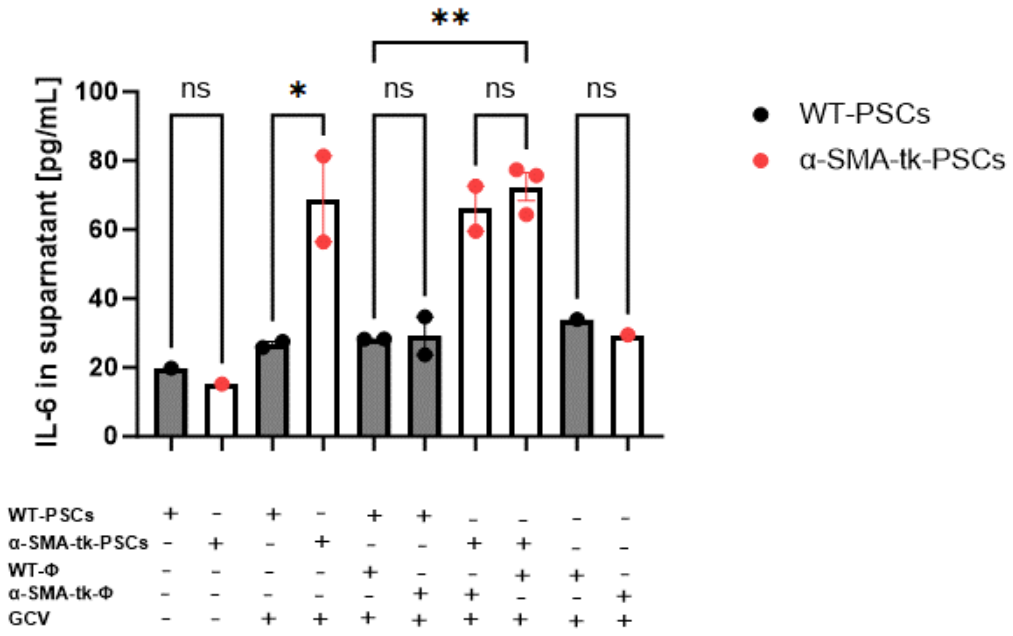

Figure 16: In vitro treatment of α-SMA+ myofibroblasts with GCV resulted in higher IL-6 level. *PSCs and macrophages were co-cultured with and without GCV (5µM) for 3 days. Elevated IL-6 release in supernatant was observed in α-SMA-tk-PSCs. Macrophages cultured with α-SMA-tk-PSCs also showed higher IL-6 level. One-way ANOVA, was performed for statistical calculations and $p < 0.05$ was considered statistically significant. Values are represented as mean (n=1) mean ± SEM (n =3).*

3.5 Influence of α-SMA+ myofibroblasts depletion on CP

3.5.1 Reduction in α-SMA+ myofibroblasts population in α-SMA-tk animals

It is well known that activated α-SMA+ myofibroblasts contribute to the development of pancreatic fibrosis by secreting ECM proteins and different cytokines [86]. In CP experiments, I performed the duct ligation and started the GCV treatment after three days of surgery when the acute phase was nearly over, and I followed up the animals for 14 and 28 days *(figure 17A)*. In the pancreas of healthy animals, only ductal cells stain positive for α-SMA, but 14 and 28 days after ligation, activated PSC or α-SMA+ myofibroblasts significantly increased, which were quantified using QuPath software *(figure 17B)*. GCV treatment led to a remarkable reduction of α-SMA+ myofibroblasts in α-SMA-tk animals compared to WT animals at both 14 and 28 days time points, as expected. I found that α-SMA-tk animals had 56% less α-SMA+ cells in

comparison to WT animals after 28 days. The efficiency and specificity of the α-SMA-tk animals were well characterized by LeBleu et al., Additionally, we confirmed that the expression of α-SMA remained unaffected in the smooth cells of the small intestine (*figure 17C).*

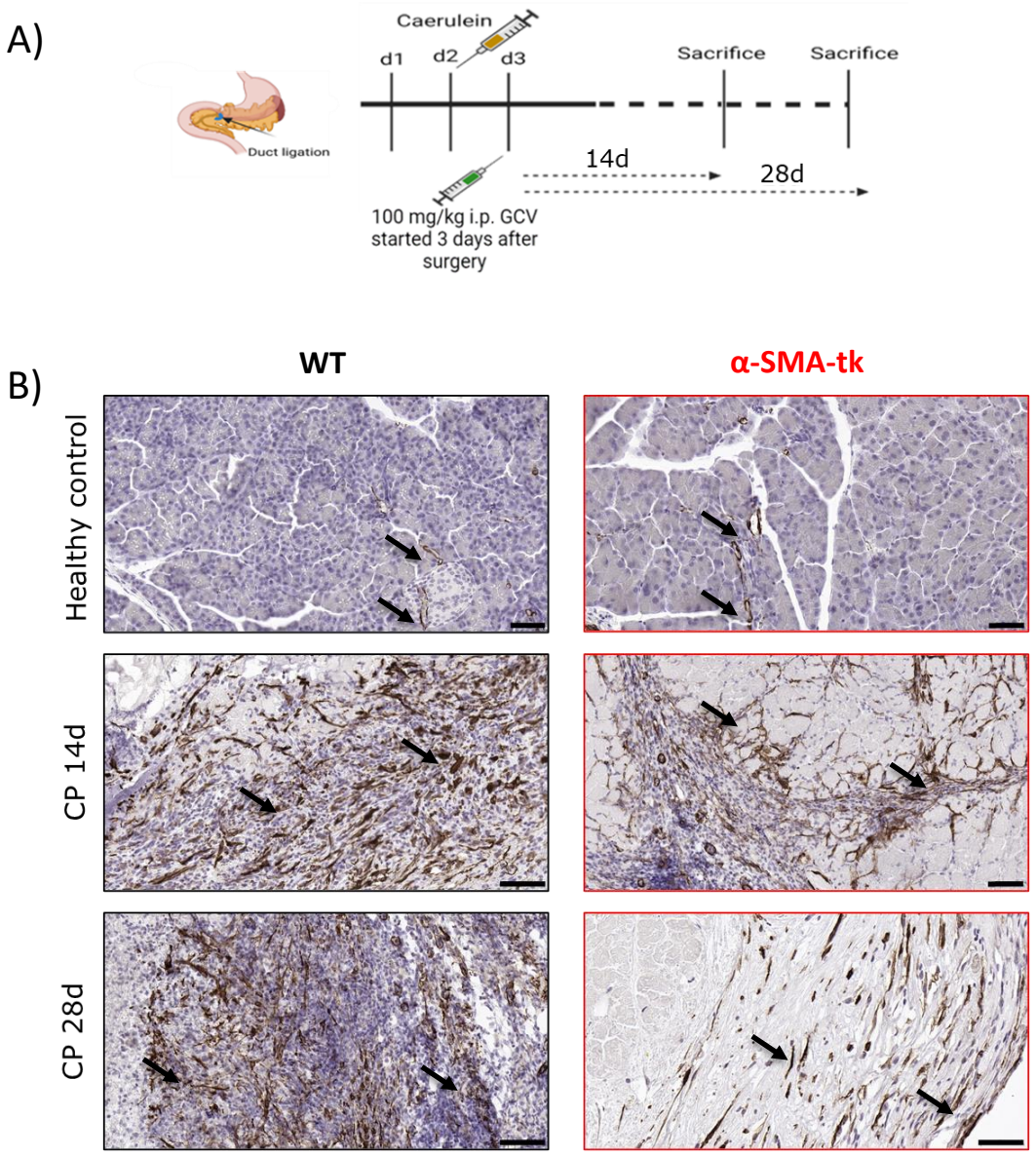

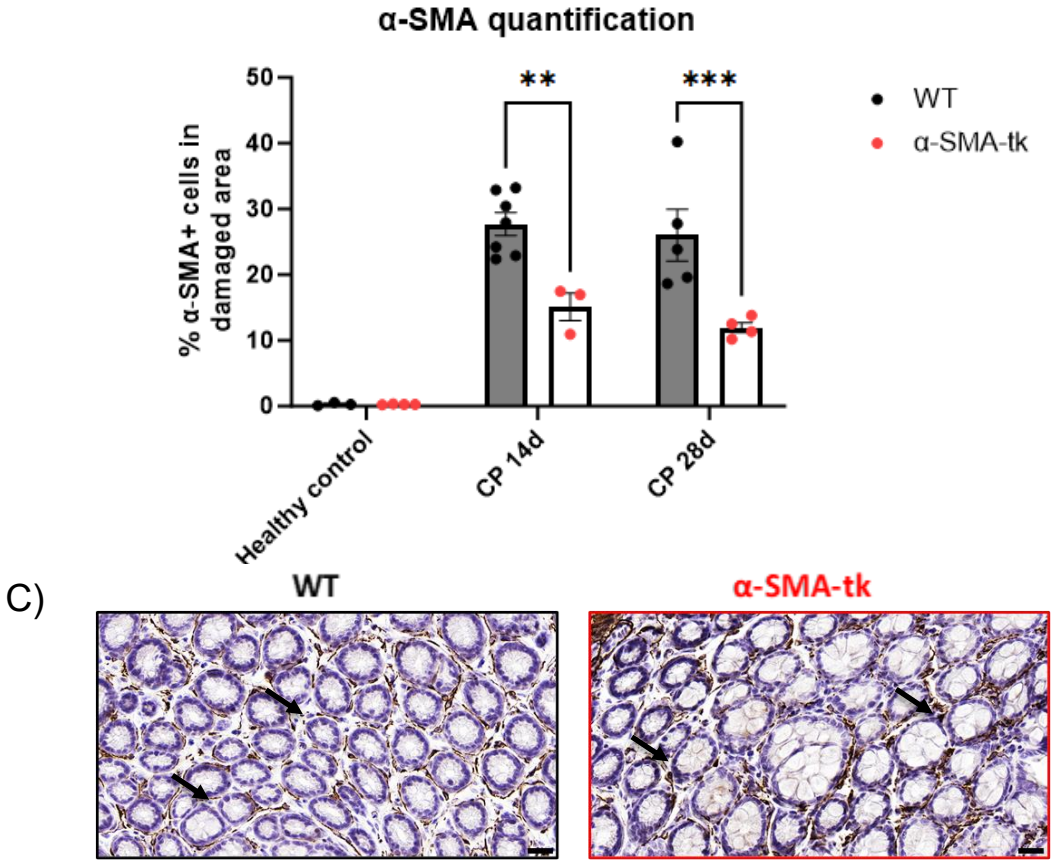

Figure 17: Reduced expression of α-SMA+ myofibroblasts in α-SMA-tk animals in CP. A) *CP was induced through duct ligation and administering a single caerulein injection (50 µg/kg) after 48h of surgery. GCV (100 mg/kg, i.p.) treatment was started three days after the surgery and continued till the end of the experiments. Animals were sacrificed at 14 days and 28 days timepoints started from day of surgery.* ***B)*** *α-SMA IHC staining was performed, which showed significant reduction of α-SMA+ myofibroblasts in α-SMA-tk animals at both time points of CP.* ***C)*** *The small intestine exhibited no changes in α-SMA expression, suggesting that under normal α-SMA promoter activity, α-SMA expression remains unaltered in healthy organs. Mixed-effects model followed by Bonferroni multiple comparison test was performed for statistical calculations, and $p < 0.05$ was considered statistically significant. Values are represented as mean ± SEM (n = 3-7).*

3.5.2 α-SMA+ myofibroblasts reduction leads to reduction of fibrosis in α-SMA-tk animals

In CP, the number of α-SMA+ myofibroblasts reduced significantly in α-SMA-tk animals. To know, whether the reduction of α-SMA+ myofibroblasts translates to a reduction in fibrosis or not, I performed PSFG staining that differentiates collagen and non-collagen parts. After the staining, I quantified the fibrosis using automated pre-trained QuPath algorithms. I observed a

reduction in pancreatic fibrosis at both time points in α-SMA-tk animals, which reached statistical significance at 28 days (33% less in comparison to WT animals) *(figure 18).*

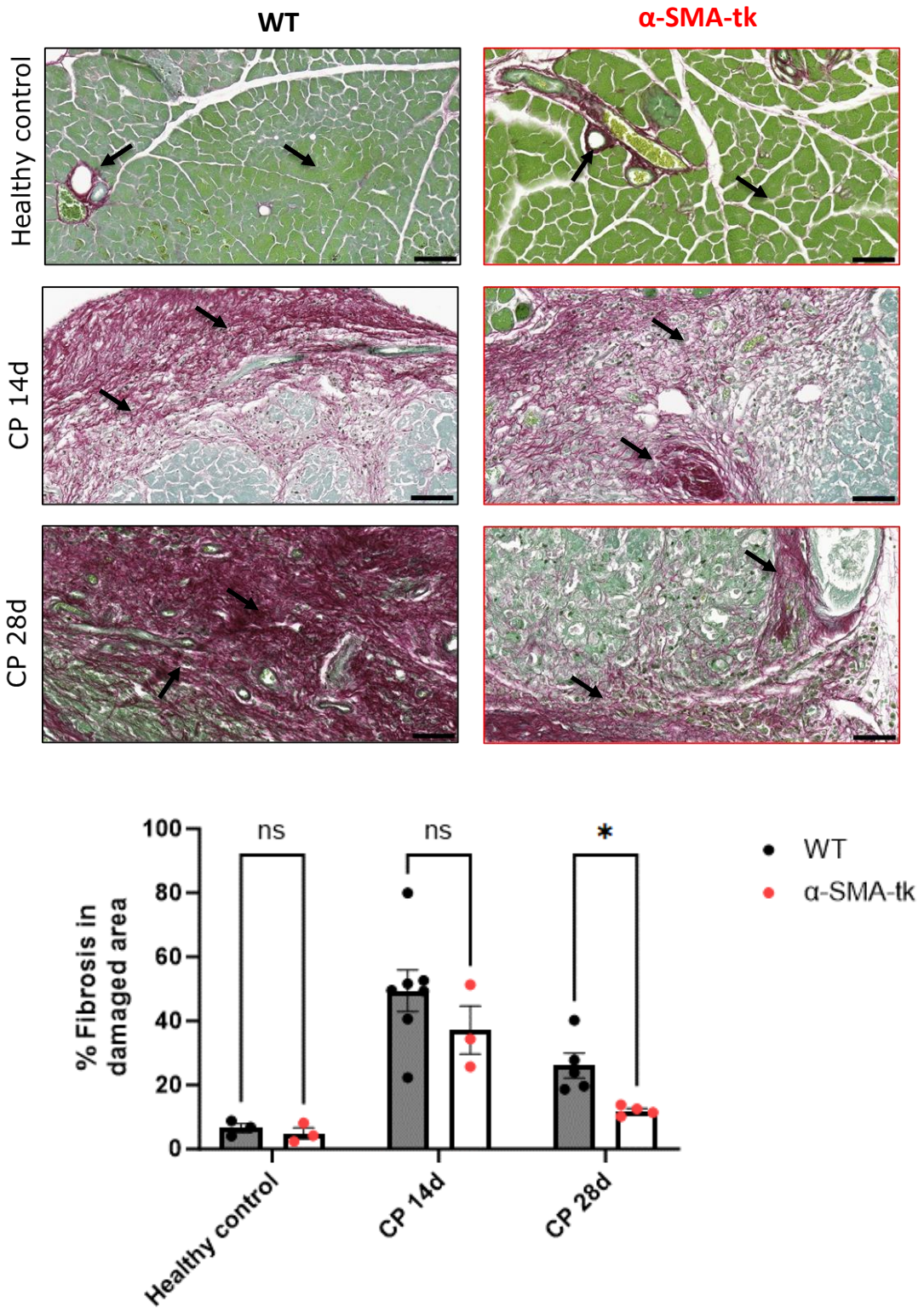

Figure 18: Depletion of α-SMA+ myofibroblasts led to fibrosis reduction in CP. *CP was induced through duct ligation and a single caerulein injection (50 µg/kg) after 48h of surgery.*

Treatment with GCV (100 mg/kg, i.p.) was initiated three days post-surgery and injected until the end of the experiments. Animals were sacrificed on day 14 and day 28 from the day of surgery. PSFG staining was performed to assess the fibrosis. PSFG staining showed reduction of fibrosis in α-SMA+ myofibroblasts depleted animals at both timepoints and was significant at 28 days of CP. Mixed-effects model followed by Bonferroni multiple comparison test was performed for statistical calculations, and $p < 0.05$ was considered statistically significant. Values are represented as mean ± SEM (n = 3-7).

3.5.3 Reduction of α-SMA+ myofibroblasts in CP caused more weight loss

Sarcopenia and weight loss are classical clinical features associated with CP [87]. My hypothesis was that the reduction of fibrosis would result in an improvement of global CP outcome parameters. During CP in animals, the body weight of all animals was assessed at least weekly using the digital scale. Notably, I found that α-SMA-tk animals experienced significant weight loss when compared to WT animals at 14 and 28 days *(figure 19)*.

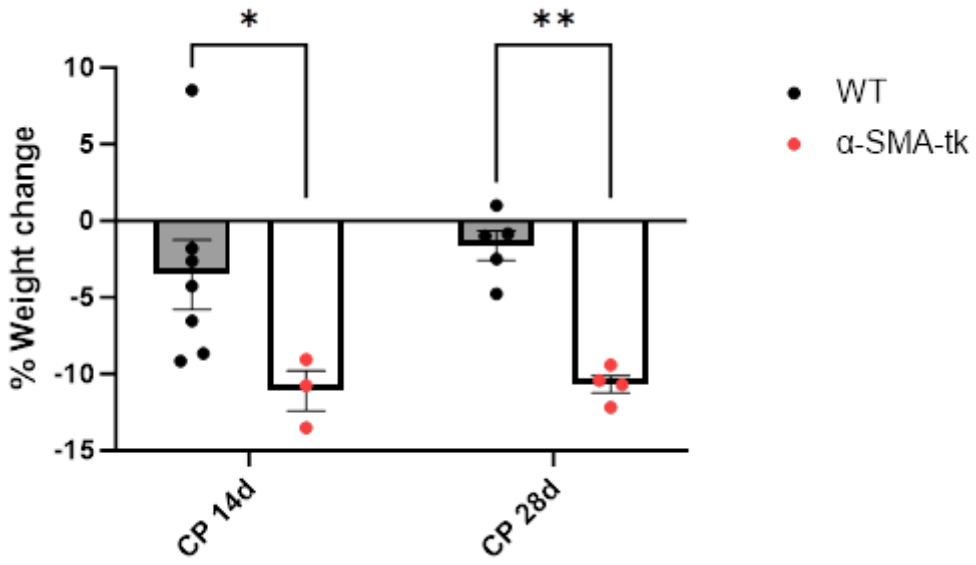

Figure 19: Influence of α-SMA+ myofibroblasts depletion on body weight in CP. *The severity of CP was assessed in the mouse model. Animals' body weights were noted every week, and relative weight changes throughout the entire experiments were calculated. After 14 and 28 days, a significant body weight difference was observed between WT and α-SMA-tk animals. Mixed-effects model followed by Bonferroni multiple comparison test was performed for statistical calculations, and $p < 0.05$ was considered statistically significant. Values are represented as mean ± SEM (n = 3-7).*

3.5.4 Effect of α-SMA+ myofibroblasts depletion in CP-associated endocrine and exocrine functions

In clinical settings, patients with CP who are losing weight often suffer from exocrine or endocrine pancreatic insufficiency, requiring pancreatic enzyme replacement therapy (PERT) and antidiabetics [88]. In animals with pancreatic duct ligation, I estimated blood glucose levels every week after fasting animals for 12h using a digital glucometer. I observed slightly better glucose control in α-SMA-tk animals in comparison with WT animals at 28 days of experiments, thus excluding gross changes in glycemic control as a reason for weight loss (*figure 20A*). Moreover, to assess the exocrine insufficiency, I estimated the fecal elastase activity in stool samples collected from each individual animal in both groups. To my surprise, I did not observe relevant differences between groups and fecal elastase activity remained unchanged in CP, likely due to the functional reserve of the remnant pancreas (*figure 20B).*

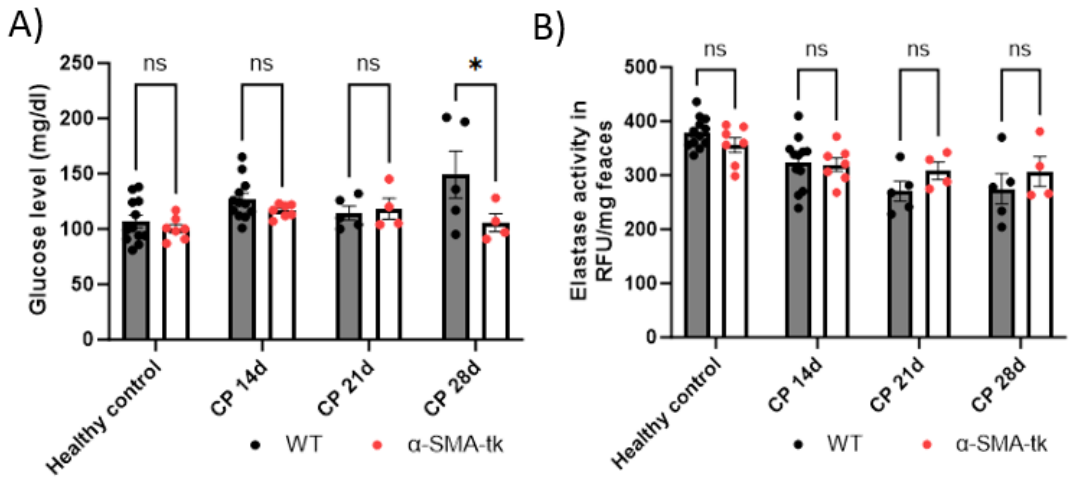

Figure 20: Influence of α-SMA+ myofibroblasts depletion on endocrine and exocrine functions in CP. *CP was induced by duct ligation followed by a single caerulein injection (50 µg/kg) after 48h of surgery. Treatment with GCV (100 mg/kg, i.p.) was initiated three days post-surgery and continued till the end of experiments. Animals were sacrificed at day 14 and day 28 from the day of surgery.* ***A)*** *Weekly fasted glucose was estimated, α-SMA-tk animals showed better glucose control.* ***B)*** *Weekly fecal elastase activity was determined and α-SMA+ myofibroblasts depleted animals did not show any changes for fecal elastase activity. Mixed-effects model followed by Bonferroni multiple comparison test was performed for statistical*

calculations and $p < 0.05$ was considered statistically significant. Values are represented as mean ± SEM (n = 3-11).

3.5.5 Depletion of α-SMA+ myofibroblasts results in increased pain sensitivity in α-SMA-tk animals

Patients suffering from CP experience severe chronic pain and its relief is one of the main therapeutic targets [89]. The role of α-SMA+ myofibroblasts has never been explored in the context of pain in CP. In my experimental study, I used two different methods to assess the pain associated with CP in the pancreatic duct ligation model. Firstly, I assessed the pain using an open field test, which captures voluntary movements for 5 minutes in a neutral environment. A reduction in movement was interpreted as a result of pain in the context of painful conditions such as pancreatitis. I found that α-SMA-tk animals were experiencing more pain, as indicated by shorter distances traveled in comparison to WT animals during the entire period of CP *(figure 21)*, however, the changes did not reach statistical significance.

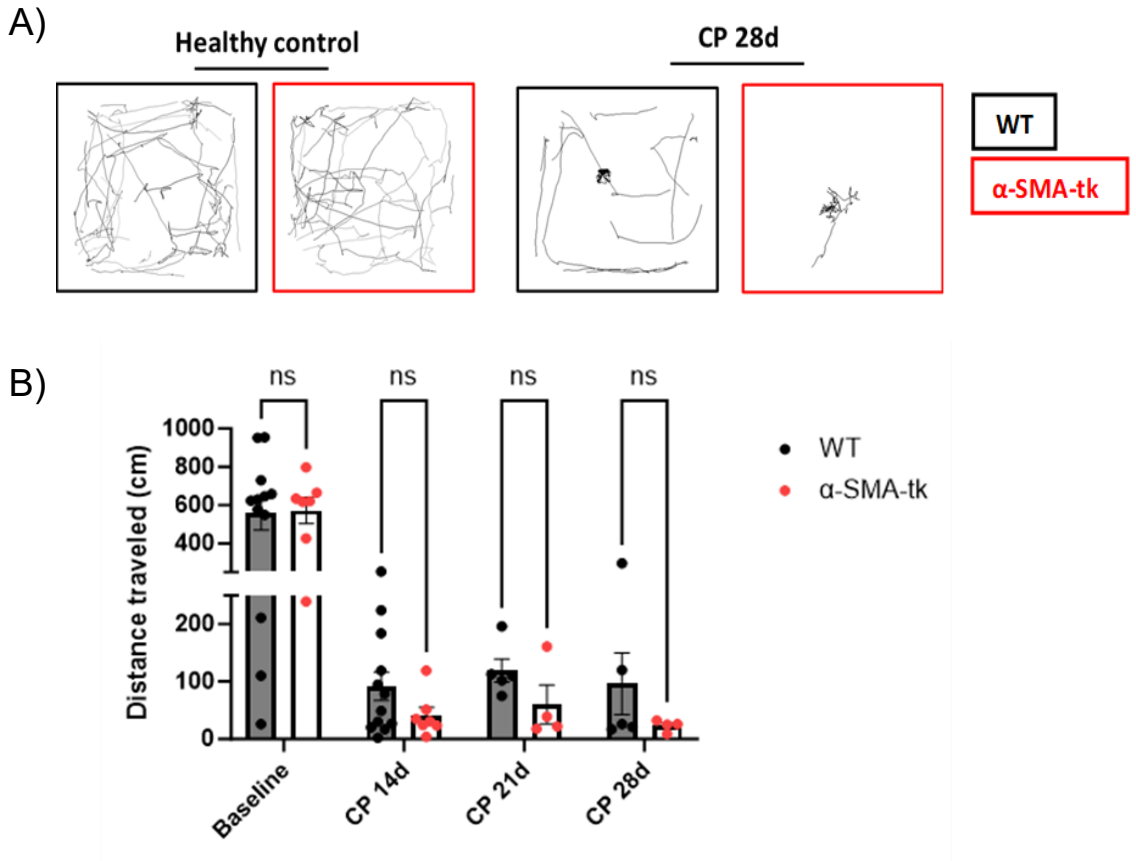

***Figure 21: CP-associated pain severity was assessed using open field test**. **A)** Grid showing the free path movement of animals in pre-defined area over 5 minutes. **B)** Open field analysis showed increased pain sensitivity in α-SMA-tk animals, as evident by less travel movements in 5 minutes. Mixed-effects model followed by Bonferroni multiple comparison test was performed for statistical calculations and $p < 0.05$ was considered statistically significant. Values are represented as mean ± SEM (n = 3-11).*

Secondly, I performed a pain behavioral experiment using vFrey filament test. I stimulated the upper abdominal wall with standardized polymeric filaments and measured the animals`reactions on an ordinal scale. A number indicates a stronger physical reaction to a standardized mechanical stimulus and is interpreted as an increase in pain sensitivity in an area exposed to a painful condition such as pancreatitis. In line with open field test, I noticed a stronger score, meaning more referred pain in α-SMA-tk animals. With the increased strength of filaments, the response was significantly higher in α-SMA-tk animals in contrast to WT animals *(figure 22).*

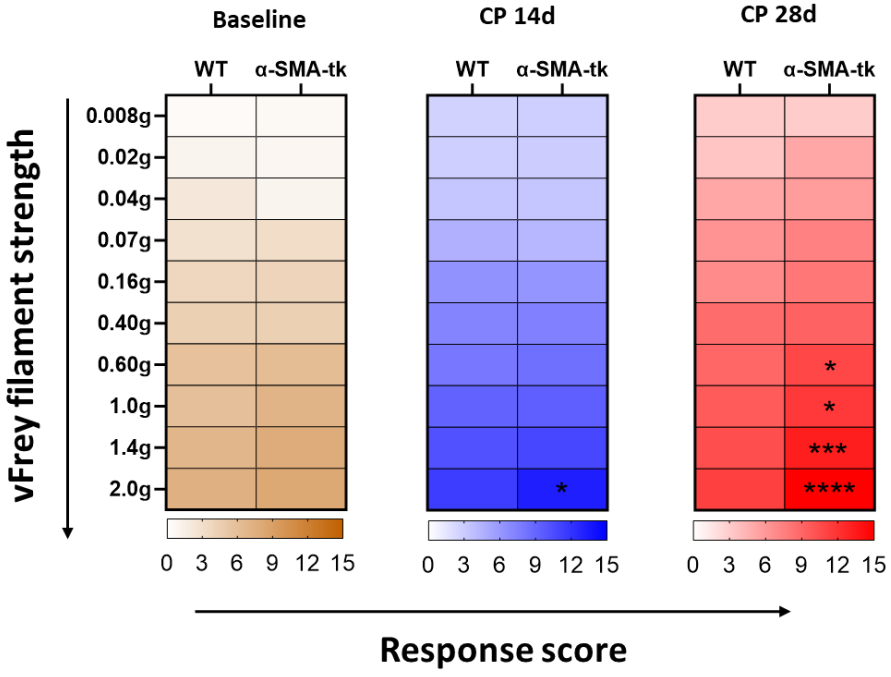

***Figure 22: Pain assessment using vFrey filament test in CP.** The severity of CP-associated pain was also confirmed using vFrey filament test to measure abdominal withdrawal responses. α-SMA-tk animals showed pronounced sensitivity to vFrey filaments as read-out for pain-related abdominal hypersensitivity in comparison to WT animals. Mixed-effects model followed by Bonferroni multiple comparison test was performed for statistical calculations,*

and p < 0.05 was considered statistically significant. Values are represented as mean ± SEM (n = 3-11).

3.5.6 α-SMA+ myofibroblasts depletion causes more nerve expression

As I was curious if there was a morphological correlation to the behavioral changes in pain testing, I performed the nerve staining using PGP9.5 antibody, which is a pan-neuronal marker. I found that α-SMA-tk animals had a more pronounced innervation in comparison to WT at 28 days timepoint. These nerves had a trend towards higher diameters in α-SMA-tk, indicating swelling and sprouting of sensory nerve endings *(figure 23).*

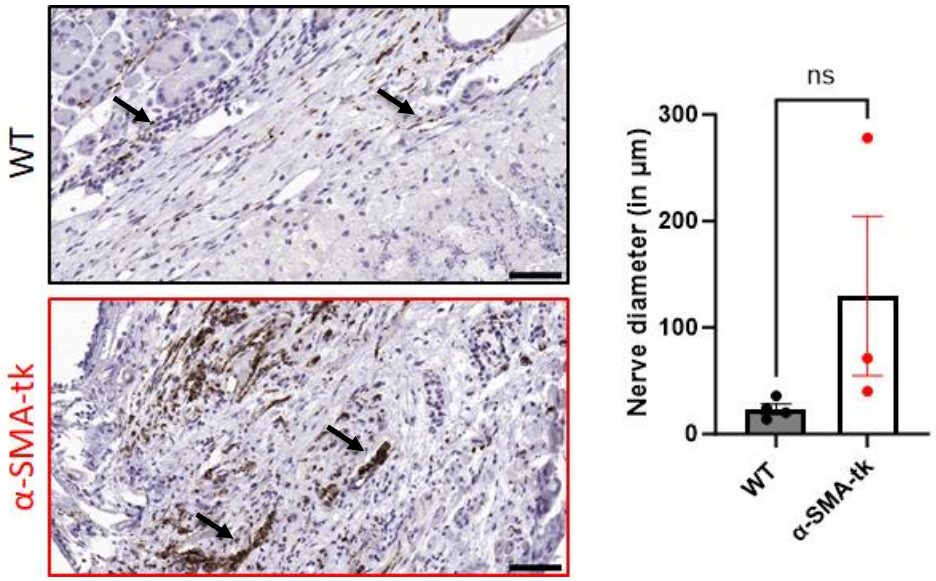

Figure 23: The severity of pain associated with CP was assessed in α-SMA-tk animals. *Pancreas tissue sections were stained with PGP9.5 using IHC. α-SMA-tk animals had more pronounced nerve expression at 28 days timepoint, and these nerves had more nerve diameter. Unpaired t-test was performed for statistical calculations, and p < 0.05 was considered statistically significant. Values are represented as mean ± SEM (n = 3-4).*

4. Discussion

To date, there is no clinically approved drug for the specific treatment of pancreatitis. Pancreatic stellate cells (PSCs) are present in the pancreas in a non-activated, quiescent state and are believed to be involved in maintaining homeostasis in the organ. After activation, PSCs start expressing α-SMA (alpha-smooth muscle actin) and acquire a myofibroblasts-like phenotype. In their activated state, PSCs (α-SMA+ myofibroblasts) act as immunomodulators and profibrogenic. So far, no one has explored how the α-SMA+ myofibroblasts influence the severity of pancreatitis directly. So, the present study aimed to explore how the α-SMA+ myofibroblasts influence the severity of pancreatitis. In this study, using α-SMA-tk transgenic animals, I explored the impact of depleting α-SMA+ myofibroblasts in both acute pancreatitis (AP) and chronic pancreatitis (CP). The findings of my study indicated that depleting α-SMA+ myofibroblasts during AP increased IL-6-driven systemic inflammation, contributing to lung damage. In CP, depletion of α-SMA+ myofibroblasts significantly reduced pancreatic fibrosis. However, this reduction in fibrosis did not improve the disease severity. Instead, I found that the reduction of α-SMA+ myofibroblasts resulted in increased weight loss regardless of exocrine and endocrine functions. Moreover, α-SMA+ myofibroblasts ablation increased pain sensitivity in α-SMA-tk animals.

4.1 Early depletion of α-SMA+ myofibroblasts increases the early humane endpoint without affecting pancreatic damage

I induced the AP in mice using pancreatic duct ligation followed by a single injection of caerulein after 24h of pancreatic duct ligation. I noticed that depleting α-SMA+ myofibroblasts in the early acute phase increased the occurrence of an early humane endpoint within 24h of caerulein injection. To study the severity and reason for acute lethality associated with AP in α-SMA-tk animals, I delayed the caerulein injection by 24h, which improved the survival of α-

SMA-tk animals. In my follow-up experiments, I sacrificed the animals after 12h, 24h, and 48h of caerulein injection. Serum lipase is commonly used as a diagnostic marker for AP in conjunction with radiological modalities [106]. I found that α-SMA-tk and WT animals had a sharp rise in serum lipase activity, depicting the successful development of the pancreatitis model. However, there was no difference in serum lipase activity between both groups.

During AP, premature activation of intracellular proteases in acinar cells leads to cellular damage. Disease severity is determined by the type of cell death, such as necrosis, apoptosis, autophagy, necroptosis, or pyroptosis [18]. I found severe histological damage in pancreatic tissue, characterized by tissue necrosis, edema, vacuolization, and inflammation, reflecting the disease's characteristics. Using Niedrau scoring method, I did not find any difference in terms of pancreatic damage between WT and α-SMA-tk animals. Damaged pancreatic acinar cells release a variety of proinflammatory mediators, including cytokines, chemokines, and damage-associated molecular patterns (DAMPs). These mediators play a crucial role in attracting and activating immune cells. Experimental mouse model of AP led to recruitment of immune cells to the pancreas in response to injury. These immune cells consist of both innate types, such as neutrophils, macrophages, dendritic cells, mast cells, and NK cells, as well as adaptive immune cells [80]. I quantified the total immune cells and macrophage populations in the damaged pancreatic tissue in AP, but I did not find any changes between both groups. Immune cells also secrete inflammatory cytokines and mediators, instigating local inflammation within the pancreas and potentially triggering a refractory systemic inflammatory response or impacting multiple organs [90, 91]. IL-6, a strong proinflammatory cytokine, is one of the most common mediators that is elevated in the early acute phase. I noticed higher IL-6 activity in pancreatic tissue in α-SMA-tk animals, but there was no significant difference between both groups. Early humane endpoint in α-SMA-tk animals is quite intriguing as it occurred without a noticeable difference in pancreatic tissue damage. These findings point toward other crucial factors, such

as systemic immune response syndrome (SIRS) and compensatory anti-inflammatory response (CARS), influencing the disease severity in AP in α-SMA-tk animals. Overall, in AP, I did not find any difference in terms of pancreatic tissue damage between both groups, demonstrating the severity in the early acute phase was not driven by the local pancreatic damage. My results imply that during the first 48h of pancreatitis, α-SMA+ myofibroblasts are not involved in the extent of local pancreatic injury or the local inflammatory response.

4.2 α-SMA+ myofibroblasts depletion result in severe proinflammatory response leading to lung damage

Severe pancreatic necrosis results in the release of massive amounts of cytokines that generate a strong systemic immune response, which often leads to MODS. Lungs are the most commonly affected and the reason for death in AP patients [12]. About one-third of patients with severe pancreatitis develop either acute lung injury (ALI) or acute respiratory distress syndrome (ARDS). This results in significant health complications and accounts for roughly 60% of pancreatitis-related fatalities within the first week of disease development in the elderly population [92]. To explore the reason behind the early humane endpoint in α-SMA-tk animals, I assessed lung injury. Interestingly, I found that α-SMA-tk animals had more pronounced lung damage and damaged alveolar structure evident by reduced alveolar space. Excessive leukocyte recruitment to the lungs is an imperative pathophysiological attribute of AP. Myeloperoxidase (MPO) forms an integral part of neutrophil-induced inflammation and is considered as a marker for systemic inflammation primarily associated with neutrophil infiltration and, to a lesser extent, from monocytes. Kumar *et al.* have reported that elevated levels of MPO are closely associated with severity in AP [93]. I harvested the lungs from WT and α-SMA-tk animals and determined the MPO levels. I observed significantly elevated levels of MPO in α-SMA-tk animals, depicting the reason for severe lung damage. One of the possible reasons for

this could be a more severe systemic inflammatory response triggered by AP in the absence of α-SMA+ myofibroblast. This led to increased lung damage seen in α-SMA+ myofibroblast-depleted mice. Pancreatic α-SMA+ myofibroblasts are essential for tissue repair and fibrosis, and they modulate inflammation during the healing process [94, 95]. Their depletion might have disrupted this equilibrium, resulting in a more intense inflammatory response that extended to the lungs. Another possible explanation for the increased lung damage might be that α-SMA+ myofibroblasts contribute to tissue integrity and controlling inflammatory mediators. In the absence of their stabilizing effects, the released proinflammatory cytokines impact distant organs such as the lungs. This cytokine storm could lead to increased lung permeability and damage. This indicates that α-SMA+ myofibroblasts may have a protective role in balancing the proinflammatory reactions in AP and depleting them causes an uncontrolled loop of inflammatory mediators.

4.3 Lung damage is driven by IL-6 mediated systemic inflammation in α-SMA-tk animals

MODS is often driven by systemic cytokine storm that mediates proinflammatory response. Different cytokines such as interleukin-6 (IL-6), interleukin (IL-17), and tumor necrosis factor-α (TNF-α) are released from the necrotic pancreas that hypersensitize the immune response. IL-6 is released by T cells, B cells, macrophages, and fibroblasts in acute inflammation. It plays a pivotal role in stimulating the acute phase, promoting inflammation, and regulating immune cell differentiation [96]. IL-17 is primarily produced by Th17 cells that drive proinflammatory response by neutrophil recruitment and activation [97]. TNF-α plays a central role in inflammatory responses and is mainly produced by activated macrophages but also can be produced by T-cells, NK-cells, and fibroblasts [98]. IL-6 is highly upregulated in the AP and associated with lung injury in both experimental mouse models of AP and patients with AP. Clinically, it

is used as a marker to diagnose pulmonary injuries [12, 14]. Zhang *et al.*, have shown IL-6 mediated lung damage in AP mouse model and reversal of lung damage using inhibitors of IL-6 trans-signaling [85]. I also observed the sharp rise of systemic IL-6 levels in my AP mouse model, which was significantly higher both in the lungs and serum samples of α-SMA-tk animals, linking IL-6 response directly to the depletion of α-SMA-expressing cells. In the pancreas lysates of matched animals, I found a similar pattern showing modestly increased levels of IL-6 in α-SMA-tk animals in contrast with WT animals. The possible reason for lower pancreatic levels of IL-6 in comparison to lung and serum samples of α-SMA-tk animals may be due to protein degradation by pancreatic proteases. α-SMA+ myofibroblasts may act as a key regulator of the inflammatory response in pancreatitis. In the absence of α-SMA+ myofibroblasts, the imbalance between proinflammatory and anti-inflammatory mediators generates a strong immune response. The findings of my study suggest that α-SMA+ myofibroblasts are modulating the release or inhibition of IL-6 release from their own or other immune cells. In the absence of α-SMA+ myofibroblasts, the inhibitory loop may become unrestricted, causing severe SIRS. The resulting higher level of IL-6 led to severe systemic injury, causing lung damage. Whether the IL-6-release induced by loss of α-SMA+ myofibroblasts alone is responsible for increased severity and lung damage, needs to be answered by a rescue experiment using specific inhibitors of IL-6 trans-signaling and neutralizing antibodies, which were beyond the scope of my thesis.

Macrophages play an indispensable role in the pathological conditions observed during AP. Macrophages secrete a large number of proinflammatory cytokines, particularly IL-6, chemokines, and growth factors, which aggravate the inflammatory cascade. They recruit a large number of other inflammatory cells that further worsen the disease condition. Moreover, macrophages initiate and propagate the systemic impairment observed in AP, and it has been shown

that macrophages and PSCs crosstalk and modulate each other's functions. In response to macrophages' inflammatory cascade, α-SMA+ myofibroblasts release TGF-β and other factors, leading to macrophages' polarization towards a proinflammatory phenotype. With macrophages secreting matrix metalloproteinases (MMPs) and tissue inhibitors of metalloproteinases (TIMPs), this bidirectional signaling affects extracellular matrix (ECM) remodeling and modifies α-SMA+ myofibroblasts activity and fibrosis progression. The interactions between different cell types are further regulated by direct cell-cell contact mediated by adhesion molecules, receptors, and different pathways such as IL-4/IL-13. [13, 99, 100]. Using FACS, I observed a significant increase in the F4/80+ macrophage population in isolated splenocytes of α-SMA-tk animals. However, *in vitro,* co-culture experiments of macrophages and PSCs from WT or α-SMA-tk animals revealed that PSCs from α-SMA-tk animals are the predominant source of IL-6 release and that co-culture with syngenic macrophages does not lead to further increase of IL-6. The possible explanation for this could be that different subtypes of PSCs are present in the pancreas, similar to the heterogeneity described for cancer-associated fibroblasts (CAFs), which have not yet been identified. It is becoming more widely acknowledged that cellular heterogeneity within tissues plays a crucial role in comprehending a variety of pathological conditions. Our knowledge of pancreatic diseases, such as inflammation and cancer, may be significantly improved if the pancreas has various subtypes of PSCs, each with unique functional characteristics. Öhlund *et al.,* were the first to identify two distinct populations of CAFs that are present in pancreatic ductal adenocarcinoma. myCAFs, which are fibrogenic and highly expressing α-SMA, and iCAFs subtype is characterized by inflammatory phenotype for which IL-6 positivity is a hallmark. Using organoids-based 3D co-culture of PSCs and tumor organoids, they found that PSCs acquire CAF phenotype in the tumor environment, reflecting the PSCs as a potential source of CAFs in PDAC [101].

In my study, I observed that early depletion of α-SMA+ myofibroblasts using the α-SMA-tk model has unveiled a significant proinflammatory cascade, culminating in IL-6-mediated lung injury. It suggests the presence of distinct subtypes within the PSCs population, which are α-SMA-negative but of strong immunomodulatory capacity. Selecting for these subtypes results in excessive release of IL-6. Consequently, the interaction of various PSCs subtypes becomes apparent as a key factor in the development of systemic inflammation and MODS during early severe acute pancreatitis. Single-cell analysis to further address the heterogeneity of PSCs and fibroblasts in the course of pancreatitis is underway but beyond the scope of this thesis.

4.4 Depletion of α-SMA+ myofibroblasts translates to a reduction in pancreatic fibrosis

For the first time, PSCs were discovered and isolated by Apte *et al., and* Bachem *et al.,* and soon after that, it was discovered that upon activation, they acquire a myofibroblast-like phenotype (α-SMA+ myofibroblasts) and are involved in tissue remodeling. Pancreatic fibrosis is believed to be an irreversible process and an important hallmark of CP [40, 41, 86]. Excessive or persistent fibrosis leads to tissue remodeling and replacement, impairing organ function. Thus, reducing fibrosis is thought to be a crucial therapeutic objective in the treatment of a number of chronic illnesses [102]. In the current study, I explored the influence of α-SMA+ myofibroblasts depletion for the course of CP. After ligation of the pancreatic duct in mice, gradually over the period of 2 to 4 weeks, animals developed pancreatic fibrosis due to activation of PSCs and excess deposition of ECM. Using α-SMA-tk animals, I depleted α-SMA+ myofibroblasts 3 days after duct ligation (hence, when the acute phase of inflammation had subsided). I observed a significant reduction of α-SMA+ myofibroblasts in α-SMA-tk animals as compared to WT animals. After 28 days, I observed an almost 56% reduction in α-SMA+ myofibroblasts, which matches with earlier findings reported by LeBleu *et al.,* who reported a

50-60% reduction in proliferating α-SMA+ myofibroblasts when using the same mouse model for the study of kidney fibrosis [78]. It has been the dogma for over 20 years that activated α-SMA+ myofibroblasts are the drivers of CP-related fibrosis [106], but for the first time, I am able to demonstrate that direct depletion of the α-SMA+ myofibroblasts population results in a significant reduction of pancreatic fibrosis.

4.5 Reduction of fibrosis leads to increased weight loss, not related to endocrine or exocrine pancreatic insufficiency

In clinical settings, pancreatic fibrosis is negatively correlated with quality of life and poor organ function. Whether this is causally related or just association in light of disease progression due to other factors, is unknown. Weight loss is one of the classical features in patients suffering from CP [87, 103]. An association of α-SMA+ myofibroblasts with weight loss has not been reported so far. Surprisingly, I observed that α-SMA-tk animals lost weight significantly in comparison to WT animals, indicating a more severe disease course. Therefore, in CP, the reduction of fibrosis as a result of direct depletion of α-SMA+ myofibroblasts is not beneficial, which is an important novel finding. This finding cautions the α-SMA+ myofibroblasts as a target to reduce the severity of CP. However, I do not know the exact mechanism behind the significant weight loss in α-SMA-tk animals. Weight loss is often attributed to the exocrine and sometimes endocrine insufficiency. Furthermore, fibrosis disrupts the normal pancreatic architecture by replacing the functional pancreatic tissue with a scar that obstructs the pancreatic duct. Pancreatic duct obstruction impairs acinar cell function, thus limiting enzyme secretion. The fibrotic scar can also damage islet cells, reducing their capacity to produce insulin and glucagon. This could lead to exocrine and endocrine insufficiency [88, 104, 105]. The reduction of α-SMA+ myofibroblasts or fibrosis did not influence the fecal elastase activity in α-SMA-tk animals in CP, indicating that exocrine insufficiency is indeed not the reason for

weight loss. Additionally, endocrine insufficiency has been reported in patients suffering with CP, especially as the disease advances. The development of pancreatic fibrosis compromises the endocrine function of the pancreas. During my CP experiments, I observed better-fasting glucose control in the late phase in α-SMA-tk animals. This finding suggests that the reduction of pancreatic fibrosis improves glucose regulation, which could be due to the preservation of pancreatic islet architecture. This improved tissue milieu could facilitate steady production and secretion of insulin, thereby enhancing fasted glucose levels. Additionally, in my mouse model of partial pancreatic duct ligation, next to damaged pancreatic tissue, unaffected healthy tissue remains, which may be enough to maintain the exocrine and endocrine function. This could also be the plausible reason for unchanged pancreatic functions in α-SMA-tk animals.

4.6 α-SMA+ myofibroblasts depletion elevated the pain sensitivity in CP

Chronic pain is the cardinal symptom of CP, and to improve the quality of life, pain management is one of the mainstays of treatment [7, 89]. Open field test is generally used to assess the stress, anxiety, and pain-related behavioral changes in rodents [82] and was used by me to evaluate the pain in α-SMA-tk and WT animals. It showed reduced voluntary movement in α-SMA-tk animals in comparison to WT animals, thus suggesting increased pain in α-SMA-tk animals. CP-associated pain mainly affects the abdominal area and persists during the course of the disease. Using vFrey filament test, I determined the pain sensitivity at the abdominal wall. In line with the open field test, I observed increased pain sensitivity in response to increasing filament strengths in α-SMA-tk animals. There could be multiple underlying factors for the enhanced pain sensitivity observed in α-SMA-tk animals. During CP, α-SMA+ myofibroblasts have a role in tissue remodeling and fibrosis, as seen by the excess production of ECM protein. Their depletion may cause anatomical alterations in the pancreas region, which may have impacted nerve endings and caused an increase in pain perception. Furthermore,

altered pancreatic inflammatory processes may be the cause of the heightened sensitivity to pain. Reduced α-SMA+ myofibroblasts activity may have altered the inflammatory environment and increase pain sensitivity. Changes in inflammatory signaling may be a factor in the increased sensitivity to pain, as inflammation can modulate pain-related pathways.

Nerves mediate the pain sensation in the damaged area, and increased pain correlates with the increased nerve expression at the site of injury and vice versa. Chronic inflammation causes increased nerve sprouting, which is often the case in CP [106, 107]. I found the diameter of nerve endings to be increased in the pancreas of α-SMA-tk animals. So far, there is no clear evidence that links myofibroblasts directly to chronic pain. My study in CP reflects the potential correlation of α-SMA+ myofibroblasts in chronic pain. Persistent pain and increased nerve expression are associated with nerve development, neural activity, and inflammation in CP [108, 109]. The absence of α-SMA+ myofibroblasts may have affected the infiltration of inflammatory cells in the pancreas, leading to altered nerve growth. Multiplex-immunohistochemistry or immunofluorescence staining can help identify distinct populations of cells surrounding the nerves that might contribute to increased nerve growth. GAP43, NGF, and BDNF play key roles in nerve growth and regeneration, and their gene expression analysis can be helpful in better understanding the underlying mechanisms of increased pain [110]. IL-1β, TNF-α, and IL-6 show inflammatory activity that might modulate nerve expression and growth within the pancreas. Furthermore, calcitonin gene-related peptide and Substance P are other indicators useful in evaluating pain signals [111]. By examining these indicators in serum samples, important mechanisms underlying nerve development and pain in CP can be identified. These approaches could potentially guide in directing treatment approaches to the management of chronic pain and modulating that particular indicator/factor may eventually subside the pain. Furthermore, pain reduces the capability of oral food intake [112]. I hypothesized that the increased pain sensitivity could also be the underlying reason for the weight loss that I observed

in α-SMA-tk animals. It has been reported that chronic stress directly influences the body weight in rodents. *Kuti et al.*, have shown that chronic stress limits the gain in body weight gain and reduces the lean mass in multiple stress models of rats. Increased stress causes an elevation in energy expenditure, thus reducing body weight [113]. Additionally, experiments under constant analgesia need to be performed in order to prove an association between pain and weight loss. Altogether, the present study suggests a complex role for α-SMA+ myofibroblasts in pancreatitis, impacting systemic inflammation, pancreatic fibrosis, weight loss, and pain sensitivity. Further studies are needed to elucidate the exact mechanisms through which α-SMA+ myofibroblasts influence disease outcomes and to identify potential therapeutic targets for managing pancreatitis.

5. Limitations

In this study, I used α-SMA-tk animals with BALB/c background to deplete the α-SMA+ myofibroblasts in the partial pancreatic duct ligation model of pancreatitis. In most studies related to pancreatitis, the C57BL/6 mouse strain is commonly used. However, I used a transgenic mouse model developed in the BALB/c background in my animal experiments, which could have influenced the findings. BALB/c strain has a different immune response, and comparing results with the earlier published study, which were carried out on the C57BL/6 mouse strain, can be challenging. BALB/c mice generally have increased levels of mast cells, basophils, and eosinophils, all of which are linked to allergy and Th2 responses. On the other hand, macrophages, dendritic cells, and natural killer cells are more prevalent in C57BL/6 mice. There are differences in the distribution and activation of T cells between the strains; BALB/c mice have a higher Th2 response and a prevalence of CD4+ T cells, whereas C57BL/6 mice frequently have higher CD8+ T cells and a bias toward Th1 responses [114-116]. In my current study, I used only a single mouse model of pancreatitis induction, which is partial pancreatic duct ligation. A second animal model of pancreatitis, such as caerulein-induced pancreatitis, is not used to confirm my findings. The transgenic mouse model was not pancreas-specific; a pancreas-specific model would provide a more robust approach, potentially eliminating concerns about off-target α-SMA+ myofibroblasts in other organs. To confirm the IL-6-mediated severity in the early acute phase, treatment with IL-6 inhibitors or IL-6 blockers is missing. Moreover, the study was conducted only in experimental animal models, and no human specimens were used. To understand and translate my findings, exploratory experiments should be carried out using sera and tissue samples from AP and CP patients.

6. Conclusions and future directions

Depleting α-SMA+ myofibroblasts in the early acute phase caused a more severe systemic immune response, resulting in the early humane endpoint. α-SMA+ myofibroblasts depletion caused IL-6 mediated lung damage in α-SMA-tk animals. However, IL-6 inhibitors-based rescue experiments should be performed for confirmation to elucidate further mechanisms behind severe immune responses in acute pancreatitis (AP). This strategy may help identify whether IL-6 is a key driver of the observed immune reaction, providing insights into potential therapeutic interventions. In chronic pancreatitis (CP), α-SMA+ myofibroblasts ablation reduced pancreatic fibrosis but increased weight loss and pain sensitivity in α-SMA-tk animals. However, how α-SMA+ myofibroblasts influence cachexia or weight loss and nerve expression in CP should be explored to get mechanistic insights. For future experiments, a metabolic cage can be used to track the feeding patterns of α-SMA-tk animals, allowing for detailed analysis of their eating habits. This approach can yield valuable insights into the underlying reasons for weight loss in these animals. Additionally, studies with concurrent analgesic therapy can be carried out to assess the effect on pain behavior in α-SMA-tk mice. This experiment can contribute to a better understanding of the pain response in these animals by determining if analgesics can mitigate the observed pain symptoms.

References

1. Szatmary, P., et al., *Acute Pancreatitis: Diagnosis and Treatment.* Drugs, 2022. **82**(12): p. 1251-1276.
2. Gu, H., et al., *Necro-inflammatory response of pancreatic acinar cells in the pathogenesis of acute alcoholic pancreatitis.* Cell death & disease, 2013. **4**(10): p. e816-e816.
3. Surbatovic, M. and S. Radakovic, *Tumor necrosis factor-α levels early in severe acute pancreatitis: is there predictive value regarding severity and outcome?* Journal of Clinical Gastroenterology, 2013. **47**(7): p. 637-643.
4. Dambrauskas, Z., et al., *Value of the different prognostic systems and biological markers for predicting severity and progression of acute pancreatitis.* Scandinavian journal of gastroenterology, 2010. **45**(7-8): p. 959-970.
5. Heckler, M., et al., *Severe acute pancreatitis: surgical indications and treatment.* Langenbeck's archives of surgery, 2021. **406**: p. 521-535.
6. Abu-Zidan, F., M. Bonham, and J. Windsor, *Severity of acute pancreatitis: a multivariate analysis of oxidative stress markers and modified Glasgow criteria.* British journal of surgery, 2000. **87**(8): p. 1019-1023.
7. Jaber, S., et al., *Guidelines for the management of patients with severe acute pancreatitis, 2021.* Anaesthesia Critical Care & Pain Medicine, 2022. **41**(3): p. 101060.
8. Walkowska, J., et al., *The pancreas and known factors of acute pancreatitis.* Journal of Clinical Medicine, 2022. **11**(19): p. 5565.
9. Yuan, S., E.L. Giovannucci, and S.C. Larsson, *Gallstone disease, diabetes, calcium, triglycerides, smoking and alcohol consumption and pancreatitis risk: Mendelian randomization study.* NPJ genomic medicine, 2021. **6**(1): p. 27.
10. Saluja, A., et al., *Early intra-acinar events in pathogenesis of pancreatitis.* Gastroenterology, 2019. **156**(7): p. 1979-1993.
11. Mayerle, J., et al., *Genetics, cell biology, and pathophysiology of pancreatitis.* Gastroenterology, 2019. **156**(7): p. 1951-1968. e1.
12. Garg, P.K. and V.P. Singh, *Organ failure due to systemic injury in acute pancreatitis.* Gastroenterology, 2019. **156**(7): p. 2008-2023.
13. Sendler, M., et al., *NLRP3 inflammasome regulates development of systemic inflammatory response and compensatory anti-inflammatory response syndromes in mice with acute pancreatitis.* Gastroenterology, 2020. **158**(1): p. 253-269. e14.
14. Glaubitz, J., et al., *Immune response mechanisms in acute and chronic pancreatitis: strategies for therapeutic intervention.* Frontiers in Immunology, 2023. **14**: p. 1279539.
15. Lilly, A.C., I. Astsaturov, and E.A. Golemis, *Intrapancreatic fat, pancreatitis, and pancreatic cancer.* Cell Mol Life Sci, 2023. **80**(8): p. 206.
16. Makhija, R. and A.N. Kingsnorth, *Cytokine storm in acute pancreatitis.* Journal of hepato-biliary-pancreatic surgery, 2002. **9**: p. 401-410.
17. Bhatia, M., et al., *Inflammatory mediators in acute pancreatitis.* The Journal of Pathology: A Journal of the Pathological Society of Great Britain and Ireland, 2000. **190**(2): p. 117-125.
18. Abdolmohammadi, K., et al., *Mesenchymal stem cell-based therapy as a new therapeutic approach for acute inflammation.* Life Sciences, 2023. **312**: p. 121206.
19. Glaubitz, J., et al., *Immune response mechanisms in acute and chronic pancreatitis: strategies for therapeutic intervention.* Frontiers in Immunology, 2023. **14**: p. 1279539.
20. Mayerle, J., *A novel role for leucocytes in determining the severity of acute pancreatitis.* Gut, 2009. **58**(11): p. 1440-1441.

21. Mahajan, U.M., et al., *Molecular, Biochemical, and Metabolic Abnormalities of Acute Pancreatitis.* The Pancreas: An Integrated Textbook of Basic Science, Medicine, and Surgery, 2023: p. 155-163.

22. Yang, Z.w., X.x. Meng, and P. Xu, *Central role of neutrophil in the pathogenesis of severe acute pancreatitis.* Journal of cellular and molecular medicine, 2015. **19**(11): p. 2513-2520.

23. Strzepa, A., K.A. Pritchard, and B.N. Dittel, *Myeloperoxidase: A new player in autoimmunity.* Cellular immunology, 2017. **317**: p. 1-8.

24. Merz, T., et al., *H2S in acute lung injury: a therapeutic dead end (?).* Intensive Care Medicine Experimental, 2020. **8**(1): p. 1-16.

25. Zhou, M.T., et al., *Acute lung injury and ARDS in acute pancreatitis: mechanisms and potential intervention.* World J Gastroenterol, 2010. **16**(17): p. 2094-9.

26. Stojanovic, B., et al., *The emerging roles of the adaptive immune response in acute pancreatitis.* Cells, 2023. **12**(11): p. 1495.

27. Oberholzer, A., C. Oberholzer, and L.L. Moldawer, *Sepsis syndromes: understanding the role of innate and acquired immunity.* Shock, 2001. **16**(2): p. 83-96.

28. Wu, J., et al., *Macrophage phenotypic switch orchestrates the inflammation and repair/regeneration following acute pancreatitis injury.* EBioMedicine, 2020. **58**.

29. Ahmad, R.S., et al., *Immune cell modulation of the extracellular matrix contributes to the pathogenesis of pancreatic cancer.* Biomolecules, 2021. **11**(6): p. 901.

30. Chan, L.K., et al., *Functional IKK/NF-κB signaling in pancreatic stellate cells is essential to prevent autoimmune pancreatitis.* Communications Biology, 2022. **5**(1): p. 509.

31. Xue, J., et al., *Alternatively activated macrophages promote pancreatic fibrosis in chronic pancreatitis.* Nat Commun, 2015. **6**: p. 7158.

32. Glaubitz, J., et al., *In mouse chronic pancreatitis CD25+FOXP3+ regulatory T cells control pancreatic fibrosis by suppression of the type 2 immune response.* Nature Communications, 2022. **13**(1): p. 4502.

33. Wilson, J.S., R.C. Pirola, and M.V. Apte, *Stars and stripes in pancreatic cancer: role of stellate cells and stroma in cancer progression.* Frontiers in physiology, 2014. **5**: p. 52.

34. Pethő, Z., et al., *Acid-base homeostasis orchestrated by NHE1 defines the pancreatic stellate cell phenotype in pancreatic cancer.* JCI insight, 2023. **8**(19).

35. Hegyi, P., Z. Szakács, and M. Sahin-Tóth, *Lipotoxicity and cytokine storm in severe acute pancreatitis and COVID-19.* Gastroenterology, 2020. **159**(3): p. 824-827.

36. Pham, A. and C. Forsmark, *Chronic pancreatitis: review and update of etiology, risk factors, and management.* F1000Research, 2018. **7**.

37. Kleeff, J., et al., *Chronic pancreatitis.* Nature reviews Disease primers, 2017. **3**(1): p. 1-18.

38. Singh, V.K., D. Yadav, and P.K. Garg, *Diagnosis and Management of Chronic Pancreatitis: A Review.* Jama, 2019. **322**(24): p. 2422-2434.

39. Ramsey, M.L., D.L. Conwell, and P.A. Hart, *Chronic pancreatitis.* Yamada's Textbook of Gastroenterology, 2022: p. 1602-1615.

40. Apte, M., et al., *Periacinar stellate shaped cells in rat pancreas: identification, isolation, and culture.* Gut, 1998. **43**(1): p. 128-133.

41. Bachem, M.G., et al., *Identification, culture, and characterization of pancreatic stellate cells in rats and humans.* Gastroenterology, 1998. **115**(2): p. 421-432.

42. Friedman, S.L., *Hepatic stellate cells: protean, multifunctional, and enigmatic cells of the liver.* Physiol Rev, 2008. **88**(1): p. 125-72.

43. Apte, M.V. and J.S. Wilson, *Alcohol-induced pancreatic injury.* Best Pract Res Clin Gastroenterol, 2003. **17**(4): p. 593-612.

44. Vonlaufen, A., et al., *Pancreatic stellate cells: partners in crime with pancreatic cancer cells.* Cancer research, 2008. **68**(7): p. 2085-2093.

45. McCarroll, J.A., et al., *Vitamin A inhibits pancreatic stellate cell activation: implications for treatment of pancreatic fibrosis.* Gut, 2006. **55**(1): p. 79-89.

46. Luttenberger, T., et al., *Platelet-derived growth factors stimulate proliferation and extracellular matrix synthesis of pancreatic stellate cells: implications in pathogenesis of pancreas fibrosis.* Laboratory investigation, 2000. **80**(1): p. 47-55.

47. Mews, P., et al., *Pancreatic stellate cells respond to inflammatory cytokines: potential role in chronic pancreatitis.* Gut, 2002. **50**(4): p. 535-541.

48. Phillips, P., et al., *Rat pancreatic stellate cells secrete matrix metalloproteinases: implications for extracellular matrix turnover.* Gut, 2003. **52**(2): p. 275-282.

49. Masamune, A., et al., *Pancreatic stellate cells express Toll-like receptors.* Journal of gastroenterology, 2008. **43**(5): p. 352-362.

50. Shimizu, K., et al., *Cytokines and peroxisome proliferator-activated receptor γ ligand regulate phagocytosis by pancreatic stellate cells.* Gastroenterology, 2005. **128**(7): p. 2105-2118.

51. Apte, M., et al., *Pancreatic stellate cells are activated by proinflammatory cytokines: implications for pancreatic fibrogenesis.* Gut, 1999. **44**(4): p. 534-541.

52. Schneider, E., et al., *Identification of mediators stimulating proliferation and matrix synthesis of rat pancreatic stellate cells.* American Journal of Physiology-Cell Physiology, 2001. **281**(2): p. C532-C543.

53. Haber, P.S., et al., *Activation of pancreatic stellate cells in human and experimental pancreatic fibrosis.* The American journal of pathology, 1999. **155**(4): p. 1087-1095.

54. Apte, M.V. and J.S. Wilson, *Alcohol-induced pancreatic injury.* Best Practice & Research Clinical Gastroenterology, 2003. **17**(4): p. 593-612.

55. Vonlaufen, A., et al., *The role of inflammatory and parenchymal cells in acute pancreatitis.* The Journal of Pathology: A Journal of the Pathological Society of Great Britain and Ireland, 2007. **213**(3): p. 239-248.

56. Nomiyama, Y., et al., *High glucose activates rat pancreatic stellate cells through protein kinase C and p38 mitogen-activated protein kinase pathway.* Pancreas, 2007. **34**(3): p. 364-372.

57. Skipworth, J., et al., *pancreatic renin–angiotensin systems in health and disease.* Alimentary pharmacology & therapeutics, 2011. **34**(8): p. 840-852.

58. Jonitz, A., B. Fitzner, and R. Jaster, *Molecular determinants of the profibrogenic effects of endothelin-1 in pancreatic stellate cells.* World Journal of Gastroenterology: WJG, 2009. **15**(33): p. 4143.

59. Aoki, H., et al., *Cyclooxygenase-2 is required for activated pancreatic stellate cells to respond to proinflammatory cytokines.* American Journal of Physiology-Cell Physiology, 2007. **292**(1): p. C259-C268.

60. Apte, M., R. Pirola, and J. Wilson, *Pancreatic stellate cells: a starring role in normal and diseased pancreas.* Frontiers in physiology, 2012. **3**: p. 344.

61. Mews, P., et al., *Pancreatic stellate cells respond to inflammatory cytokines: potential role in chronic pancreatitis.* Gut, 2002. **50**(4): p. 535-41.

62. Norman, J., *The role of cytokines in the pathogenesis of acute pancreatitis.* Am J Surg, 1998. **175**(1): p. 76-83.

63. Formela, L.J., S.W. Galloway, and A.N. Kingsnorth, *Inflammatory mediators in acute pancreatitis.* Br J Surg, 1995. **82**(1): p. 6-13.

64. Apte, M.V., et al., *Pancreatic stellate cells are activated by proinflammatory cytokines: implications for pancreatic fibrogenesis.* Gut, 1999. **44**(4): p. 534-41.

65. Mantovani, A., et al., *Regulation of inhibitory pathways of the interleukin-1 system.* Ann N Y Acad Sci, 1998. **840**: p. 338-51.

66. Symons, J., J. Eastgate, and G. Duff, *Interleukin 1 as an inflammatory mediator*, in *Biochemistry of Inflammation*. 1992, Springer. p. 183-210.

67. Pezzilli, R., et al., *Serum interleukin-10 in human acute pancreatitis.* Dig Dis Sci, 1997. **42**(7): p. 1469-72.

68. Gloor, B., et al., *Mechanism of increased lung injury after acute pancreatitis in IL-10 knockout mice.* J Surg Res, 1998. **80**(1): p. 110-4.

69. Norman, J. *Rapid elevation of systemic cytokines during acute pancreatitis and their origination within the pancreas*. in *Surg Forum*. 1994.

70. Inagaki, T., et al., *Interleukin-6 is a useful marker for early prediction of the severity of acute pancreatitis.* Pancreas, 1997. **14**(1): p. 1-8.

71. Aoki, H., et al., *Autocrine loop between TGF-β1 and IL-1β through Smad3-and ERK-dependent pathways in rat pancreatic stellate cells.* American Journal of Physiology-Cell Physiology, 2006. **290**(4): p. C1100-C1108.

72. Michalski, C.W., et al., *Mononuclear cells modulate the activity of pancreatic stellate cells which in turn promote fibrosis and inflammation in chronic pancreatitis.* Journal of translational medicine, 2007. **5**(1): p. 1-11.

73. Andoh, A., et al., *Cytokine regulation of chemokine (IL-8, MCP-1, and RANTES) gene expression in human pancreatic periacinar myofibroblasts.* Gastroenterology, 2000. **119**(1): p. 211-219.

74. Shek, F.W.-T., et al., *Expression of Transforming Growth Factor-β1 by Pancreatic Stellate Cells and Its Implications for Matrix Secretion and Turnover in Chronic Pancreatitis.* The American Journal of Pathology, 2002. **160**(5): p. 1787-1798.

75. McLaughlin, P., *Tumour necrosis factor (TNF) and inflammation*, in *Biochemistry of Inflammation*. 1992, Springer. p. 211-223.

76. LeBleu, V.S., et al., *Origin and function of myofibroblasts in kidney fibrosis.* Nat Med, 2013. **19**(8): p. 1047-53.

77. Heyman, R.A., et al., *Thymidine kinase obliteration: creation of transgenic mice with controlled immune deficiency.* Proc Natl Acad Sci U S A, 1989. **86**(8): p. 2698-702.

78. LeBleu, V.S., et al., *Origin and function of myofibroblasts in kidney fibrosis.* Nature medicine, 2013. **19**(8): p. 1047-1053.

79. Kruger, N.J., *The Bradford method for protein quantitation.* The protein protocols handbook, 2009: p. 17-24.

80. Wilden, A., et al., *Mobilization of CD11b+/Ly6chi monocytes causes multi organ dysfunction syndrome in acute pancreatitis.* Frontiers in Immunology, 2022. **13**: p. 991295.

81. Sendler, M., et al., *Complement component 5 mediates development of fibrosis, via activation of stellate cells, in 2 mouse models of chronic pancreatitis.* Gastroenterology, 2015. **149**(3): p. 765-776. e10.

82. Gould, T.D., D.T. Dao, and C.E. Kovacsics, *The open field test.* Mood and anxiety related phenotypes in mice: Characterization using behavioral tests, 2009: p. 1-20.

83. Barrot, M., *Tests and models of nociception and pain in rodents.* Neuroscience, 2012. **211**: p. 39-50.

84. Niederau, C., L.D. Ferrell, and J.H. Grendell, *Caerulein-induced acute necrotizing pancreatitis in mice; protective effects of Proglumide Benzotript, and Secretin.* Gastroenterology, 1985. **88**(5): p. 1192-1204.

85. Zhang, H., et al., *IL-6 trans-signaling promotes pancreatitis-associated lung injury and lethality.* The Journal of clinical investigation, 2013. **123**(3): p. 1019-1031.

86. Apte, M., R. Pirola, and J. Wilson, *The fibrosis of chronic pancreatitis: new insights into the role of pancreatic stellate cells.* Antioxidants & redox signaling, 2011. **15**(10): p. 2711-2722.

87. Armbrecht, U., *[Chronic pancreatitis: weight loss and poor physical performance - experience from a specialized rehabilitation centre].* Rehabilitation (Stuttg), 2001. **40**(6): p. 332-6.

88. Diéguez-Castillo, C., et al., *Role of Exocrine and Endocrine Insufficiency in the Management of Patients with Chronic Pancreatitis.* J Clin Med, 2020. **9**(6).

89. Pasricha, P.J., *Unraveling the mystery of pain in chronic pancreatitis.* Nature reviews Gastroenterology & hepatology, 2012. **9**(3): p. 140-151.

90. Peng, C., Z. Li, and X. Yu, *The role of pancreatic infiltrating innate immune cells in acute pancreatitis.* International journal of medical sciences, 2021. **18**(2): p. 534.

91. Xue, J., V. Sharma, and A. Habtezion, *Immune cells and immune-based therapy in pancreatitis.* Immunologic research, 2014. **58**: p. 378-386.

92. Manohar, M., et al., *Chronic Pancreatitis Associated Acute Respiratory Failure.* MOJ Immunol, 2017. **5**(2).

93. Kumar, S., et al., *Role of serum myeloperoxidase in patients of acute pancreatitis: a sole prognostic marker.* Journal of the American College of Surgeons, 2014. **219**(4): p. e108-e109.

94. Hinz, B., *Formation and Function of the Myofibroblast during Tissue Repair.* Journal of Investigative Dermatology, 2007. **127**(3): p. 526-537.

95. Hinz, B., et al., *The Myofibroblast: One Function, Multiple Origins.* The American Journal of Pathology, 2007. **170**(6): p. 1807-1816.

96. Leser, H.G., et al., *Elevation of serum interleukin-6 concentration precedes acute-phase response and reflects severity in acute pancreatitis.* Gastroenterology, 1991. **101**(3): p. 782-5.

97. Li, G., et al., *Role of Interleukin-17 in Acute Pancreatitis.* Frontiers in Immunology, 2021. **12**.

98. Malleo, G., et al., *Role of tumor necrosis factor-alpha in acute pancreatitis: from biological basis to clinical evidence.* Shock, 2007. **28**(2): p. 130-40.

99. Hu, F., et al., *Macrophages in pancreatitis: Mechanisms and therapeutic potential.* Biomedicine & Pharmacotherapy, 2020. **131**: p. 110693.

100. Allawadhi, P., et al., *Novel Insights Into Macrophage Diversity During the Course of Pancreatitis.* Gastroenterology, 2021. **161**(6): p. 1802-1805.

101. Ohlund, D., et al., *Distinct populations of inflammatory fibroblasts and myofibroblasts in pancreatic cancer.* J Exp Med, 2017. **214**(3): p. 579-596.

102. Wynn, T.A. and T.R. Ramalingam, *Mechanisms of fibrosis: therapeutic translation for fibrotic disease.* Nat Med, 2012. **18**(7): p. 1028-40.

103. Robinson, S.M., et al., *Systemic inflammation contributes to impairment of quality of life in chronic pancreatitis.* Scientific Reports, 2019. **9**(1): p. 7318.

104. Hegyi, P. and O.H. Petersen, *The exocrine pancreas: the acinar-ductal tango in physiology and pathophysiology.* Reviews of Physiology, Biochemistry and Pharmacology, Vol. 165, 2013: p. 1-30.

105. Frantz, C., K.M. Stewart, and V.M. Weaver, *The extracellular matrix at a glance.* J Cell Sci, 2010. **123**(Pt 24): p. 4195-200.

106. Demir, I.E., et al., *Pain mechanisms in chronic pancreatitis: of a master and his fire.* Langenbecks Arch Surg, 2011. **396**(2): p. 151-60.

107. Olesen, S.S., et al., *Towards a neurobiological understanding of pain in chronic pancreatitis: mechanisms and implications for treatment.* PAIN Reports, 2017. **2**(6): p. e625.

108. Hiraga, S.-i., et al., *Neuroplasticity related to chronic pain and its modulation by microglia.* Inflammation and Regeneration, 2022. **42**(1): p. 15.

109. Goulden, M.R., *The pain of chronic pancreatitis: a persistent clinical challenge.* Br J Pain, 2013. **7**(1): p. 8-22.

110. Denny, B.J., *Molecular Mechanisms, Biological Actions, and Neuropharmacology of the Growth-Associated Protein GAP-43.* Current Neuropharmacology, 2006. **4**(4): p. 293-304.

111. Greco, R., et al., *Role of calcitonin gene-related peptide and substance P in different models of pain.* Cephalalgia, 2008. **28**(2): p. 114-26.

112. Malick, A., et al., *A neurohistochemical blueprint for pain-induced loss of appetite.* Proceedings of the National Academy of Sciences, 2001. **98**(17): p. 9930-9935.

113. Kuti, D., et al., *The metabolic stress response: Adaptation to acute-, repeated- and chronic challenges in mice.* iScience, 2022. **25**(8): p. 104693.

114. Fukushima, A., et al., *Genetic background determines susceptibility to experimental immune-mediated blepharoconjunctivitis: comparison of Balb/c and C57BL/6 mice.* Exp Eye Res, 2006. **82**(2): p. 210-8.

115. Sellers, R.S., et al., *Immunological Variation Between Inbred Laboratory Mouse Strains:Points to Consider in Phenotyping Genetically Immunomodified Mice.* Veterinary Pathology, 2012. **49**(1): p. 32-43.

116. Fransen, F., et al., *BALB/c and C57BL/6 Mice Differ in Polyreactive IgA Abundance, which Impacts the Generation of Antigen-Specific IgA and Microbiota Diversity.* Immunity, 2015. **43**(3): p. 527-540.

Acknowledgment

First and foremost, I want to express my deep sense of gratitude and respect to my supervisor, **Prof. Dr. med. Julia Mayerle**, Chair of the Department of Internal Medicine at the University Hospital Großhadern. Her keen interest in my research project, constant encouragement, concrete suggestions, meticulous guidance, and constructive criticism helped me at every step of my research. Our engaging discussions during lab meetings, lab retreats, hiking trips, and the APA conference were truly motivating and encouraged me to develop my interest in pancreatic disease research.

Secondly, I want to convey my heartfelt thanks to my beloved co-supervisor, **PD Dr. med. Georg Beyer**. I will always be indebted to him for his constant support, mentorship, trust in my abilities, and encouragement during frustrating times. I greatly enjoyed our critical scientific discussions, especially during the last year of my PhD when we met every Thursday morning over Indian tea. These discussions were influential in shaping my research project. I will never forget his tremendous efforts in improving my public speaking skills, which significantly enhanced my communication abilities and led me to win three distinguished research awards across three different continents.

I also want to express my gratitude to my official supervisor, **Prof. Dr. rer. nat. Sibylle Ziegler**, Head of Preclinical Research at the Department of Nuclear Medicine. Her constant input during our regular project updates helped improve the overall outcomes of my PhD research. Her welcoming nature and scientific discussions are truly admirable.

Next, I owe significant credit for my PhD thesis to **PD Dr. Ujjwal Mahajan**. His unwavering support in the lab, whether through scientific discussions or personal improvement, was truly amazing. He possesses a perfect blend of knowledge, whether it is about history, pancreatic diseases, bioinformatics, or cooking.

Running a lab group is very challenging and comes with a plethora of responsibilities and scientific expertise. Here, the front-runner and the first lady of our lab, **PD Dr. Ivonne Regel**, played an indispensable role. Words cannot adequately express her contributions in keeping the lab running smoothly. Her suggestions and discussions during my PhD journey are unforgettable.

I want to convey my thanks to **Prof. Dr. Kirsten Lauber** and Dr. Nikko Brix for their kind support for performing FACS for my project. I would like to extend my sincere thanks to my amazing lab members: Simon Gahr, Maria Escobar, Simon Sirtl, Ahmed Alnatsha, Frau Fahr (Lisa), Quan Zhou, Nicole Schreiner, Mahmood Ahmad, Didem Saka, Francesca Mendia, Tahib Habshi, Sikdar Saheri, Jianyin, Nirali Donga, Esther Weber, Julia Wolff, Klea Ricku, Song, Johannes, Nadine, Rebecca, Yongann Xue, Qi Li and entire Pancreas team.

Outside of the lab, I want to convey my special thanks to the Mahajan family for providing a homely feeling that prevented homesickness and loneliness. My deepest thanks go to my brother and friend, Mr. Mathews P. George, for his engaging discussions, encouragement, support, and care. I cherished every single moment spent with Shinson Joseph and Kevin at Buchendorf. Thanks to my entire friend circle in Munich: Deepak, Ankush Jha, Swasti, Azeem, Safal Walia, Sameera Peri, and Aparna Chiku, who made my stay in Munich joyful.

I am greatly blessed by the Almighty through my parents, who always encouraged me to work passionately and acknowledge God in every moment of life. Great thanks to my brother Sachin, who inspired me to come to Germany and whose constant support helped me to complete my PhD. I can't imagine finishing PhD without their encouragement. My cousins Mitu, Sakshi, and Gargi also contributed tremendously, helping me accomplish my PhD.

I owe my acknowledgment to the innocent animals that were major contributors to the success of my journey toward achieving my doctoral degree by sacrificing their lives. Finally, I would

like to thank from the bottom of my heart every individual who has directly or indirectly supported me in completing my doctoral journey. I am deeply thankful to Mr. Shams Tahir Khan for his thrilling crime stories, which made my lab work and time afterward truly enjoyable. It is impossible to mention everyone who has impacted this work, but I am deeply grateful to all.

I dedicate my PhD thesis and PhD title to my belated and beloved sister Ms. Shallu Allawadhi Mehndiratta. This thesis is the result of her motivation and the motivating words (कर हर मैदान फ़तेह, May you conquer every challenge) which are engraved in my mind and heart forever.

Affidavit

Affidavit

Prince
_____
Surname, first name

_____
Street

_____
Zip code, town, country

I hereby declare, that the submitted thesis entitled:

Depletion of α-SMA+ myofibroblasts aggravates pancreatitis in mice

is my own work. I have only used the sources indicated and have not made unauthorized use of services of a third party. Where the work of others has been quoted or reproduced, the source is always given.

I further declare that the dissertation presented here has not been submitted in the same or similar form to any other institution for the purpose of obtaining an academic degree.

Munich, 08.01.2025 Prince

_____ _____
Place, Date Signature doctoral candidate

Confirmation of congruency

Confirmation of congruency between printed and electronic version of the doctoral thesis

Prince

_____

Surname, first name

_____

Street

_____

Zip code, town, country

I hereby declare, that the submitted thesis entitled:

Depletion of α-SMA+ myofibroblasts aggravates pancreatitis in mice

is congruent with the printed version both in content and format.

Munich, 08.01.2025 Prince

_____ _____

Place, Date Signature doctoral candidate

List of publications

- *Sirtl S, Bretthauer K, Ahmad M, Hohmann E, Schmidt VF, **Allawadhi Prince**, Vornhülz M, Klauss S, Goni E, Vielhauer J, Orgler E, Saka D, Knoblauch M, Hofmann FO, Schirra J, Schulz C, Beyer G, Mahajan UM, Mayerle J, Zorniak M. Severity of gallstone, sludge or microlithiasis induced pancreatitis - all of the same? Pancreas. 2024 May 1. doi: 10.1097/MPA.0000000000002349. Epub ahead of print. PMID: 38696426.*
- ***Allawadhi Prince**, Beyer G, Mahajan UM, Mayerle J. Novel Insights Into Macrophage Diversity During the Course of Pancreatitis. Gastroenterology. 2021 Dec;161(6):1802-1805. doi: 10.1053/j.gastro.2021.09.049. Epub 2021 Sep 26. PMID: 34587487.*
- *Mahajan UM, Li Q, Alnatsha A, Maas J, Orth M, Maier SH, Peterhansl J, Regel I, Sendler M, Wagh PR, Mishra N, Xue Y, **Allawadhi Prince**, Beyer G, Kühn JP, Marshall T, Appel B, Lämmerhirt F, Belka C, Müller S, Weiss FU, Lauber K, Lerch MM, Mayerle J. Tumor-Specific Delivery of 5-Fluorouracil-Incorporated Epidermal Growth Factor Receptor-Targeted Aptamers as an Efficient Treatment in Pancreatic Ductal Adenocarcinoma Models. Gastroenterology. 2021 Sep;161(3):996-1010.e1. doi: 10.1053/j.gastro.2021.05.055. Epub 2021 Jun 25. PMID: 34097885.*

Conference awards

- **Deutschen Pankreasclubs e. V., Bonn-2024**

Depletion of α-SMA+ myofibroblast aggravates pancreatitis in mice
(Poster)
"Best poster award and travel grant award"

- **American Pancreatic Association at San Diego, California-2023**

Depletion of α-SMA+ myofibroblast aggravates pancreatitis in mice
(Oral)
"Young investigator award"

- **Pancreas 2023 organized by IAP-IPC at New Delhi, India-2023**

"Depletion of α-SMA+ myofibroblast aggravates pancreatitis in mice"
(Oral)
"Young investigator award"

Curriculum vitae

Prince

Date of Birth April 19th, 1995.

Education

2019-2024	Department of Internal Medicine, University of Munich (LMU), Germany.
2018-2019	Junior Research Fellow, Department of Biotechnology, Indian Institute of Technology-Roorkee, India.
2016-2018	Department of Pharmacology, Jamia Hamdard, New Delhi, India.
2012-2016	Vaish Institute of Pharmaceutical Sciences and Research, Rohtak, India.

Degrees

2018	Master of Pharmacy, Pharmacology.
2013	Bachelor of Pharmacy.

Research Experience

2019-2024	PhD Candidate, Department of Internal Medicine II, Munich University Hospital, Ludwig-Maximilians-University, Germany. Field of Research: Role of activated pancreatic stellate cells in pancreatitis.
2018-2019	Junior Research Fellow, Department of Biotechnology, Indian Institute of Technology-Roorkee, India. Field of Research: Role of lysyl oxidase enzyme in rheumatoid arthritis.
2016-2018	M. Pharmacy, Research Scholar, Department of Pharmacology, Jamia Hamdard, New Delhi, India. Field of Research: Investigated the therapeutic potential of cerium oxide nanoparticles in rheumatoid arthritis (*in vitro* and *in vivo*).

Awards

2024	Best poster and travel grant award by German Pancreatic Club.
2023	Young-investigator and travel award by American Pancreatic Association.
2024	Young-investigator award by the International Association of Pancreatology.

2023 India's best thesis award in the pharmacology category by Troikaa Pharmaceuticals- supported by DST India (Master's thesis).

Publications

- *Sirtl S, Bretthauer K, Ahmad M, Hohmann E, Schmidt VF, **Allawadhi Prince**, Vornhülz M, Klauss S, Goni E, Vielhauer J, Orgler E, Saka D, Knoblauch M, Hofmann FO, Schirra J, Schulz C, Beyer G, Mahajan UM, Mayerle J, Zorniak M. Severity of gallstone, sludge or microlithiasis induced pancreatitis - all of the same? Pancreas. 2024 May 1. doi: 10.1097/MPA.0000000000002349. Epub ahead of print. PMID: 38696426.*
- ***Allawadhi Prince**, Beyer G, Mahajan UM, Mayerle J. Novel Insights Into Macrophage Diversity During the Course of Pancreatitis. Gastroenterology. 2021 Dec;161(6):1802-1805. doi: 10.1053/j.gastro.2021.09.049. Epub 2021 Sep 26. PMID: 34587487.*
- *Mahajan UM, Li Q, Alnatsha A, Maas J, Orth M, Maier SH, Peterhansl J, Regel I, Sendler M, Wagh PR, Mishra N, Xue Y, **Allawadhi Prince**, Beyer G, Kühn JP, Marshall T, Appel B, Lämmerhirt F, Belka C, Müller S, Weiss FU, Lauber K, Lerch MM, Mayerle J. Tumor-Specific Delivery of 5-Fluorouracil-Incorporated Epidermal Growth Factor Receptor-Targeted Aptamers as an Efficient Treatment in Pancreatic Ductal Adenocarcinoma Models. Gastroenterology. 2021 Sep;161(3):996-1010.e1. doi: 10.1053/j.gastro.2021.05.055. Epub 2021 Jun 25. PMID: 34097885.*

Declaration

I hereby solemnly declare that all the information I furnish is true to the best of my knowledge and belief.

Date: 08.01.2025 Prince

Place: Munich, Germany